Published in final edited form as:
RSC Adv. 2013 ; 3(43): . doi:10.1039/C3RA42769B.

Synthesis and evaluation of fluorescent cap analogues for mRNA labelling

Marcin Ziemniak[a], **Mariusz Szabelski**[b], **Maciej Lukaszewicz**[a], **Anna Nowicka**[a], **Edward Darzynkiewicz**[a], **Robert E. Rhoads**[c], **Zbigniew Wieczorek**[b], and **Jacek Jemielity**[a,d]

[a]Division of Biophysics, Institute of Experimental Physics, Faculty of Physics, University of Warsaw, Zwirki i Wigury 93, 02-089 Warsaw, Poland [b]Department of Physics and Biophysics, University of Warmia and Mazury in Olsztyn, Oczapowskiego 4, 10-719 Olsztyn, Poland [c]Department of Biochemistry and Molecular Biology, Louisiana State University Health Sciences Center, Shreveport, Louisiana 71130-3932, USA [d]Centre of New Technologies, University of Warsaw, Zwirki i Wigury 93, 02-089 Warsaw, Poland

Abstract

We describe the synthesis and properties of five dinucleotide fluorescent cap analogues labelled at the ribose of the 7-methylguanosine moiety with either anthraniloyl (Ant) or N-methylanthraniloyl (Mant), which have been designed for the preparation of fluorescent mRNAs *via* transcription *in vitro*. Two of the analogues bear a methylene modification in the triphosphate bridge, providing resistance against either the Dcp2 or DcpS decapping enzymes. All these compounds were prepared by $ZnCl_2$-mediated coupling of a nucleotide P-imidazolide with a fluorescently labelled mononucleotide. To evaluate the utility of these compounds for studying interactions with cap-binding proteins and cap-related cellular processes, both biological and spectroscopic features of those compounds were determined. The results indicate acceptable quantum yields of fluorescence, pH independence, environmental sensitivity, and photostability. The cap analogues are incorporated by RNA polymerase into mRNA transcripts that are efficiently translated *in vitro*. Transcripts containing fluorescent caps but unmodified in the triphosphate chain are hydrolysed by Dcp2 whereas those containing a α-β methylene modification are resistant. Model studies exploiting sensitivity of Mant to changes of local environment demonstrated utility of the synthesized compounds for studying cap-related proteins.

Introduction

A characteristic feature of almost all eukaryotic mRNAs is the presence of a cap at the 5′ terminus. The cap is an unique residue composed of a 7-methylguanosine moiety connected to the mRNA body *via* a triphosphate linkage, $m^7GpppGpNp(Np)n$[1, 2]. The unusual chemical structure of the cap is pivotal for essentially all stages of mRNA metabolism: synthesis, splicing, nucleocytosolic transport, intracellular localization, translation, and turnover. The cap itself is a target for specific pyrophosphatases, such as the Dcp1/2 decapping complex and the decapping scavenger enzyme DcpS, which play a vital role in mRNA turnover. Consequently, synthetic analogues of the cap have proven to be valuable tools for investigating numerous biological processes as well as being applicable in biotechnology and medicine[3].

[†]Electronic Supplementary Information (ESI) available: [details of any supplementary information available should be included here]. See DOI: 10.1039/b000000x/

One application is the enzymatic synthesis of capped RNAs with either bacteriophage[4] or bacterial[5] RNA polymerases. However, these polymerases do not discriminate between Guo and m^{7}Guo for addition of the growing polynucleotide chain, and as a result, 30–50% of the RNAs are capped in the reverse orientation, i.e., Gpppm^{7}GpNp(Np)n[5]. This is prevented by replacing conventional cap analogues with anti-reverse cap analogues (ARCAs) that contain modifications at either the 2′- or 3′-positions of the m^{7}Guo moiety[5, 6]. mRNAs with modified caps have proven to be beneficial for both basic research and practical applications[7–13].

There are two general types of chemical modifications that can be made in the cap analogue. One is to change its properties so as to alter its biological features e.g., increasing its affinity to a certain protein or resistance to an enzymatic action[2, 7]. The second is to introduce features that allow one to monitor the cap analogue or capped mRNA in a biological system, preferably *without* altering its biological features. Introducing a fluorophore into the cap analogue is a promising approach for achieving the latter. Fluorescence is a potent technique to obtain information about the behaviour of molecules within biological systems[14, 15]. For instance fluorescence microscopy is capable of imaging the cellular distribution of macromolecules with high sensitivity[16–18], and Förster resonance energy transfer (FRET) allows one to study macromolecule dynamics and interactions[19, 20]. Recent developments in fluorescence microscopy have enabled single-molecule methods that can provide otherwise inaccessible information on statistical distribution and time trajectories[21, 22]. To date, fluorescent nucleotides have found a plethora of applications in biochemistry[23–25], molecular biology[26, 27] and nanotechnology[28, 29].

Typically, a fluorophore is composed of two or more connected aromatic rings, which are essential to shift the excitation wavelength into the visible region. In some cases, probes are large enough to interfere with binding interactions between a protein and its ligand. However, there are also a number of compact, low molecular weight dyes that can serve this purpose. Groups such as anthraniloyl (Ant), N-methylanthraniloyl (Mant) and trinitrophenyl (TNP) are environmentally sensitive fluorophores that emit a stronger signal upon binding to a target[30]. Nucleotides labelled with these tags closely mimic naturally occurring nucleotides in their interactions with molecular targets[31–33]. Typically, these fluorophores are covalently attached to one or both OH groups of the ribose ring[32]. (M)Ant-labelled nucleotides were successfully used to study the behaviour of numerous proteins, including bacterial toxins[34–37], G proteins[38] and human adenosylcyclases[39, 40]. One complication upon derivatization of ribose OH groups is formation of a mixture of 2′ and 3′ regioisomers that exist in a dynamic equilibrium[34, 41]. Nonetheless, the small size of these fluorophores makes them promising candidates for mRNA cap labelling. The synthesis of fluorescent cap analogues has been previously reported[31, 42, 43], but none have been designed to be incorporated into mRNA transcripts or modified in the phosphate chain to change their susceptibility to enzymatic degradation. The latter cap analogues have proven to be valuable for the study of cap-related processes[8, 44–47]. Combining these properties – fluorescence, the ability to be incorported into mRNA, and stability to enzymatic hydrolysis – should allow one to examine new aspects of cap-related processes both *in vivo* and *in vitro*.

We describe here a method for preparation and biochemical properties of five cap analogues, compounds **1-5,** labelled with either Ant or Mant, that are potentially useful for the study of mRNA translation, turnover, or other cellular processes involving mRNA. Due to the replacement of one bridging oxygen by a methylene moiety, compounds **3** and **4** are stable to degradation by the Dcp1/2 complex[47] and DcpS[48], respectively. Because the 2′ OH group of compound **5** is methylated, the fluorescent tag is definitively localized to the 3′ position. Hence, this analogue might be used to examine interactions with eIF4E and other cap binding proteins without any potential problems caused by migration of the fluorophore.

Results and discussion

Chemical synthesis

Five triphosphate dinucleotide cap analogues bearing either Ant or Mant fluorescent tags were prepared (Fig. 1). Two of these compounds (**1**-**2**) are derivatives of the canonical cap dinucleotide, m^7GpppG, without any modification of the phosphate chain, whereas two others (**3**-**4**) have one of the bridging oxygen atoms substituted by a methylene group. Both high performance liquid chromatography (HPLC) and mass spectrometry (MS) indicated that compounds **1**-**4** exist a mixture of two regioisomers in a dynamic equilibrium, which is consistent with previous publications on (M)Ant-labelled nucleotides[49, 50]. Compound **5** also bears a 2′-*O* methyl group on m^7G, which blocks the isomerisation and results in a defined 3′position for the Ant moiety. During syntheses of the final dinucleotides **1**-**5**, two reactions should be noted as key synthetic steps, the label attachment to nucleotide and the $ZnCl_2$-mediated coupling of two nucleotide subunits to form a dinucleotide 5′,5′-triphosphate. The synthesis of intermediates **6-10** is depicted in Scheme 1. For label attachment we applied synthetic procedures similar to those previously described for anthraniloyl-m^7GTP and *N*-methylanthraniloyl-diadenosinetetraphosphates[43, 51], but with several modifications. 7-Methylguanine-containing nucleoside mono- or diphosphates were treated with either isatoic or N-methylisatoic anhydride in aqueous solution at pH 9.5 to obtain the mononucleotide labelled with Ant or Mant, respectively. Reversed phase (RP) HPLC was used to follow the reaction progress. When m^7GDP (**11**) was treated with isatoic anhydride, both expected regioisomers of Ant-m^7GDP (**6**) were detected. However, another product emerged during the reaction progress. This side product displayed a considerably higher retention time than the expected products. Further analysis by MS revealed that it was 2′, 3′-diAnt-m^7GDP, i.e., possessing two Ant residues, presumably one each on the 2′ and 3′ OH groups. The analogous side product was observed during preparation of Mant-m^7GDP (**7**), but the observed rate of diMant-m^7GDP formation was ~2-fold slower than for diAnt-m^7GTP. The highest ratio of mono- to disubstituted product was obtained when both reagents were nearly equimolar. Specifically, 1–1.2 eq. of anhydride were added in small portions (~0.2 eq.) 5–6 times over a period of 1h. Under these conditions, the undesired side-product was ~10%. We initially attempted purification of compounds **6-10** from unreacted and doubly labelled nucleotides by applying ion-exchange chromatography, but we observed partial decomposition of the products to unlabelled substrates and free (M)Ant acid during evaporation of TEAB buffer. Furthermore, the TEA salts of **6-10** deteriorated even if stored in the cold. To reduce this loss, nucleotides **6-10** were immediately used as reactants in the coupling reactions described below.

In order to obtain intermediates **6-10** in pure and stable form for structure confirmation by NMR, we switched to another purification protocol – size exclusion chromatography on G-15 resin[43, 52]. Even though this method resulted in pure sodium salts of compounds **6-10**, size exclusion chromatography cannot be used in the overall synthesis scheme because the sodium salts are insoluble in the organic solvents used for the subsequent coupling reaction.

The key step in the preparation of compounds **1**-**5** was $ZnCl_2$-mediated coupling of two nucleotides to form a dinucleoside 5′,5′-triphosphate. One nucleotide was converted to the active P-imidazolide and the second nucleotide acted as a nucleophilic agent (**6-10**), which allowed formation of the pyrophosphate bond[53]. The reactants, products, HPLC conversion, and preparative yield of each coupling reaction are summarized in Table 1. In principle, two alternative approaches are possible for triphosphate bridge formation. In the first, a nucleotide is activated at the stage of monophosphate and then coupled to flouorophore-labelled 7-methylguanosine diphosphate or 7-methylguanosine bisphosphonate (Scheme 2). In the second, guanosine diphosphate or guanosine bisphosphonate is activated and coupled

with flourophore-labelled 7-methylguanosine monophosphate (Scheme 3). A third, theoretically possible approach is the activation of a nucleotide (mono- or diphosphate) labelled with Ant or Mant, but this was considered unlikely to succeed and was not tested. To illustrate the first route of synthesis, compounds **1** and **2** were prepared using activated GMP (GMP-Im, **15**) and either Ant-m^{7}GDP (**6**) or Mant-m^{7}GDP (**7**), respectively. Conversion to products was high in both cases: 92% for Ant-m^{7}GDP and 81% for Mant-m^{7}GDP. A similar synthetic route, coupling of Mant-m^{7}GpCH$_2$p (**9**) with **15**, was used to synthesize compound **4**, which has a methylene bridge between the β and γ phosphates. (Scheme 2). The first reactant (**9**) was synthesised by the previously described methodology of preparing Mant-labelled nucleotides starting from m^{7}GpCH$_2$p (**13**) (Scheme 1) and reacted with **15**. Compound **3**, which has a methylene bridge between the β and γ phosphates was prepared by coupling Mant-m^{7}GMP (**8**) with GpCH$_2$p-Im (**18**) (Scheme 3). **18** was prepared starting from guanosine, which was converted to GpCH$_2$p (**20**) in Yoshikawa-like phosphonylation using methylenebis(phosphonic) dichloride[54], and then **20** was converted into the phosphoroimidazolidate **18**. MS analysis demonstrated that **20** was slightly contaminated by methylenobisphosphonate, which co-eluted during ion-exchange chromatography. As a result, methylene-bis(1-imidazolyl)phosphonate was formed in the next step. This contaminant diminished the yield of coupling between **8** and **18** because of the formation of various side products such as Mant-m^{7}GppCH$_2$p or Mant-m^{7}GppCH$_2$ppm^{7}G-Mant. Despite this impediment, compound **3** was obtained with yield of 12% after two purification steps, ion-exchange and RP HPLC purification (HPLC conversion 63%). Coupling of **8** and **18** afforded compound **3** with 8% yield after a two-step purification. Compound **5** was prepared by coupling of Ant-m$_2^{7,2'\text{-}O}$GMP (**10**) with **17,** which was obtained from GDP (**19**) (Scheme 3). m$^{2'\text{-}O}$GMP was obtained from m$^{2'\text{-}O}$Guo by Yoshikawa phosphorylation. The next steps were methylation at the N7 position followed by tagging with the Ant moiety. Importantly, blocking of the 2′-OH with a methyl group effectively prevented the formation of diAnt-substituted products. This enabled us to use 1.5 eq. of isatoic anhydride in a single addition, thus shortening the reaction time. Compound **5** was prepared with 26% yield after a two-step purification.

Spectroscopic studies

Compounds **1, 2,** and **5** were selected for detailed spectroscopic studies. Fig. 2 shows electronic absorption and emission spectra recorded in phosphate buffered saline (PBS), and Table 2 summarizes the spectroscopic data. It is known that the spectroscopic properties of aminobenzoic acid derivatives depend on the amino group substituent and modification of the carboxyl group[55, 56]. Therefore, methylanthranilate (AntOMe) and methyl-*N*-methylanthranilate (MantOMe) were selected as reference probes for spectroscopic studies. The absorption and emission spectra of AntOMe and MantOMe in buffer solutions at pH 5.18 and 8.96 are shown in Fig. S1. There was no difference between the absorption and emission peaks over a pH range of 5 to 9. Quantum yields and lifetimes were also identical within experimental error (Table S1). Similarly the absorption and emission peaks of (M)Ant moieties attached to the cap did not change significantly over this pH range (Fig. 2). The absorption spectra have two maxima, at 254 and 334 nm (361 nm for compound **2**), which correspond to the absorption of the nucleobase and Ant (or Mant), respectively. Interestingly, the absorbance maximum for Ant in **1** is red-shifted 5 nm in comparison to AntOMe, and the same phenomenon occurs for the Mant-labelled compound (**2**). The broad shoulder in the absorption spectrum at 280 nm corresponds to the 7-methylguanosine moiety. That absorbance maximum exhibits pH dependence, due to the presence of the ionizable *N1* proton in m^{7}Guo. This dependence was used to calculate the pK_a of the m^{7}Guo *N1* ionization in the cap analogues. The pK_a values for compounds **1**, **2**, and **5** were 7.41, 7.42 and 7.49, respectively. These values are similar to the pK_a of the unmodified cap analogue (7.50), which indicates that introduction of these fluorescent tags does not alter

ionization of the *N1* proton of m^7Guo, an important finding since we sought to make minimal changes to the biological properties of the cap analogues. Interestingly, the incorporation of Ant or Mant moieties into the cap structure increased their fluorescence intensities and lifetimes. This suggests a close interaction between the fluorescent probe and hydrophobic parts of the nucleotide, since such interactions would be expected to change the polarity in the vicinity of the fluorophore. Emission spectra of cap analogues recorded in methanol or ethanol revealed a considerable increase in quantum yields, which is similar to the results obtained with the reference probes. The contribution of the short lifetime component was significantly decreased if the cap analogue was dissolved in methanol. This component vanished totally in ethanol and only the long lifetime could be detected. This is likely due to stabilisation of the excited state by the solvent, which diminishes the rate of non-radiative decay of the excited fluorophore and leads to an increase in fluorescence lifetime. A similar increase influorescence intensity could also possibly occur upon binding to cap-recognising proteins due to changes in local polarity. Similar observations on quantum yield augmentation and lifetime extension were reported by Turchiello *et al.*[57].

The photostability of compounds **1**, **2**, and **5** was assessed with time-based fluorescence measurements. The compounds were exposed to light for 9 h to induce photobleaching. We found less than a 3% loss of fluorescence intensity. Furthermore, there were no detectable changes in the shape of excitation spectra before and after exposure to light (data not shown).

NMR studies

The fact that compounds **1-4** exist as equilibrium mixtures of 2′ and 3′ (M)Ant regioisomers is reflected in their ^{1}H NMR spectra[49, 50]. Some protons display different chemical shifts depending on whether they are assigned to the 2′ or 3′ regioisomer, which allows one to calculate the ratio between isomers using the ^{1}H NMR spectrum of the configurationally stable compound **5** as a reference. In the case of Ant-m^7GpppG, the 2′ and 3′ isomer made up 32% and 68%, respectively. The distribution of isomers was similar for Mant-m^7GpppG (42% and 58%) (Table S2). These findings are in general agreement with previous studies of (M)Ant-labelled mononucleotides. Thus, the stacking interactions between m^7G and G rings in dinucleotide cap analogues have a minimal impact on the distribution between 2′ and 3′ isomers. Interestingly, the ratios of these regioisomers for compounds **1** and **2** are similar to the ratios of fluorescence lifetimes, suggesting that the short and long lifetime are derived from the 3′ and 2′ regioisomers, respectively. However, it should be noted that compound **5**, which has a fixed position for the Ant moiety, also shows two different fluorescence lifetimes (Table 2). Hence, the assumption that observed lifetimes correlate with different conformations of the ribose ring is a more likely explanation for this phenomenon. The conformation of the ribose ring of cap analogue **5** was analyzed in terms of a dynamic equilibrium between two favored puckered conformations N and S[58, 59]. The percentages of the two conformers were calculated using experimentally determined vicinal coupling constants $^3J_{H,H}$ for protons in the sugar moiety, which has been reported previously[61]. Using the assigned coupling constants, the fractions of N and S conformers were determined to be 0.37 and 0.63, respectively. These values correlate well with the contributions of fluorescence lifetimes originating from different excited states (see Table 2). However, in the case of compounds **1** and **2**, the populations of S and N conformers do not correlate with the calculated fluorescence lifetimes contributions (Table S3). This implies that in the case of compounds with 2′/3′-shifting of (M)Ant groups, the observed lifetime contributions may stem from a combination of different conformations of sugar moiety and the regioisomerism. We are currently investigating this phenomenon further with molecular modeling methods.

In vitro synthesis of capped RNAs

We examined the efficiencies for incorporation of compounds 1-5 into short (48 nt) RNA transcripts by T7 RNA polymerase. Transcripts synthesised in the presence of compounds 1-5 were subjected to polyacrylamide gel electrophoresis (PAGE), and capping efficiency was measured after exposure of the gel to autoradiography. The capping efficiencies for compounds **1**-**5** are presented in Table 3. The capping efficiency for the parent compound $m^{7,3'}$-*O*GpppG was 72±2%. It appears that both Ant and Mant moieties are well tolerated by T7 polymerase since the capping efficiency for cap analogues **1**-**5** was only slightly lower. A similar observation has been reported for biotin-labelled cap analogues [60].

Translation *in vitro*

The translational properties of mRNAs containing compounds **1**-**5** were assessed using a rabbit reticulate lysate (RRL) translation system programmed with firefly luciferase mRNA Fig. 3 and Table 3). Due to a significant percentage of reverse-incorporated cap analogue, i.e., Gpppm^{7}GpNp(Np)n, the translational efficiency of mRNA capped with m^{7}GpppG was considerably lower than that of mRNAs capped with ARCAs. Since compounds **1**-**5** are functional equivalents of ARCAs, the results indicated that the presence of the (M)Ant tag slightly impedes recognition of the cap by the translational machinery. The translational efficiencies of mRNAs containing compounds **3** and **4,** which possess the methylene modification, were lower than those of their unmodified counterparts **1**, **2**, and **5** (Fig. 3 and Table 3), which agrees with previous findings.

Decapping assays

Short capped transcripts (48 nt) were subjected to incubation with the Dcp1/2 decapping complex from Schizosaccharomyces pombe (SpDcp1/2) in order to investigate their susceptibility to hydrolysis. This enzyme complex cleaves the pyrophosphate bond between the α and β phosphates yielding m7GDP and the decapped RNA. The capped and decapped (or uncapped) RNAs migrate differently on electrophoresis. The mobility of the ~30% of molecules that are uncapped is similar to that of decapped mRNA12.

Transcripts synthesised in the presence of compounds **1**-**5** were incubated for 0, 15, or 30 min with recombinant SpDcp1/2 and subjected to electrophoresis. The amount of RNA was then measured by autoradiography (Fig. 4). The upper band contains capped RNA and the lower band contains uncapped and decapped RNA. The percentage of capped RNA is calculated from ratio of the radioactivity of the upper band to the total radioactivity contained in the upper and lower bands. Decapping is expressed as the decrease in this percentage (Table 3). The presence of uncapped RNA is taken into account in the calculation of the extent of decapping by subtracting a no-enzyme control. RNAs capped with compounds **1**, **2**, **4** were cleaved by SpDcp1/2, but the rate of decapping was slightly slower for fluorescent mRNAs compared to mRNAs capped with reference analogues (m^{7}GpppG and $m_2^{7,3'}$-*O*GpppG)[49]. The transcript capped with cap analogue compound **3**, bearing the α-β methylene modification, was not susceptible to SpDcp1/2, which is in agreement with previous studies[45, 47].

Sensitivity of fluorescence of the Mant labeled cap to changes of local environment

We tested wether the sensitivity of Mant label to changes in local polarity may be used for studying cap enzymatic degradation or protein binding. In the first model experiment, compound **2** was used as a substrate for hDcpS enzyme. DcpS hydrolyzes the residual m^{7}GpppN$_n$ cap structures remaining after the cytoplasmic 3′→5′ degradation of mRNA by the exosome, cleaving between the γ and β phosphates and releasing m^{7}GMP from capped (oligo)nucleotides[61]. DcpS is also involed with pre-mRNA splicing and has recently been

identified as a therapeutic target for spinal muscular atrophy[62]. We found that upon the action of hDcpS Mant-m^{7}GpppG is converted to Mant-m^{7}GMP and GDP. The fluorescence intensity of Mant-m^{7}GMP is lower than the intensity of the dinucleotide substrate (**2**), probably due to loss of interactions between the label and hydrophobic parts of the second nucleoside (guanosine). After complete cleavage of **2** by DcpS the fluorescence of the sample was diminished to ~60% of the initial intensity. This enabled monitoring the DcpS-catalyzed reaction progress by spectrofluorymetry (Fig. 5). Three reactions were performed at 200, 100 or 50 nM substrate concentration (Fig 5). Notably, even at the lowest concentration the fluorescence changes were sufficient to monitor reaction progress. For comparison, the non-labeled cap analogue, m^{7}GpppG, also displays a weak fluorescence arising from m^{7}G moiety. The fluorescence of m^{7}GpppG is increased after cleavage by DcpS to m^{7}GMP and GDP, due to loss of stacking interactions between the two nucleotides, and this can also be exploited for reaction progress monitoring (Fig. 5A). However, in the case of m^{7}GpppG reaction can be followed at concentrations not lower than 1 μM. Hence, due to introduction of Mant moiety the sensitivity of the assay could be increased by ~20 fold. It is known that the presence of substituents at the 2′ or 3′ positions of m^{7}G ribose moiety decreases the affinity of cap analogues for DcpS[63]. In agreement with that, the presence of Mant label attached to ribose of m^{7}G residue decreased the reaction rate compared to unmodified cap cap analogue. However, due to small size of the Mant label, the compound could still serve as a relatively good substrate for DcpS. In our opinion, this results suggest that the Mant labeled cap analog **2** may be used as fluorescent molecular probe for assaying potential DcpS inhibitors. The conventional, HPLC-based assays are much more time-consuming, require high amounts of materials due to higher detection limits and are limited by problems with overlapping signals from the substarte or products and the inhibitor.

Another possible application of cap analogues **1**-**5** is to study protein-ligand interactions. As it was mentioned before, a number of studies indicated that fluorescence intensity of (M)Ant-labelled compounds is enhanced upon binding to a target protein. In a model experiment we used eukaryotic translation initiation factor 4E (eIF4E), an important component of translation initiation complex, which directly binds the mRNA cap structure. The interaction of cap with eIF4E constitutes an important cellular mechanism of regulation of gene expression at the translational level[64]. Morover, it has been established that eIF4E is overexpressed in many cancer cells and it has been demonstrated in several studies that preventing interaction of eIF4E with other constituents of the translation initiation complex may inhibit tumor growth[65]. We performed a “reverse titration” experiment, in which to a given concentration of compound **2** increasing amounts of eIF4E protein were added.

We observed that the Mant fluorescence intenstity was increased to up to 2-fold along with the increasing amount of eIF4E (Fig. 6). In contrast, if MantOMe was titrated by eIF4E no fluorescence augmentation could be noted (Fig. S3). The fluorescence enhancement can be attributed to the increase of local hydrophobicity upon cap binding to eIF4E. Hence, the results suggest that the prepared cap analogues can be applied to study protein-cap interactions. Interestingly, we also found that changes in compound **2** fluorescence properties may also be monitored upon excitation of Trp residues in eIF4E (Fig S4), which also may be used to study this protein.

Conclusions

The fluorescently labeled analogues described here constitute a novel class of molecular probes that are potentially useful for a variety of biochemical and biophysical techniques. The cap itself demonstrates weak innate fluorescence, but due to its low quantum yield, hence it cannot be used for most fluorescence-based techniques.

An advantage of these compounds is their relatively straightforward and inexpensive preparation compared to some other molecular probes. Several biophysical features should make them particularly favorable for fluorescence-based biochemical assays: i) high quantum yields, ii) an excitation wavelength that is outside the absorbance range of proteins, and iii) striking photostability. Several biochemical features should make them favourable for *in vitro* studies of processes involving mRNA: i) ability to be incorporated into mRNA by RNA polymerases, ii) ability of fluorescent mRNAs to be recognized by the translational machinery, and iii) enzymatic susceptibility to decapping enzymes. Furtheremore, it was confirmed that the fluorescence of (M)Ant-labelled cap analogues is influenced by the polarity of the microenvironment and hence a useful read-out for protein-cap interactions. Introduction of the stabilizing α-β methylene modification to the polyphosphate bridge creates various opportunities to study decapping in vitro by means of fluorescence based assays. For instance, rate of the loss of fluorescence anisotropy after decapping initiation would be a measure of decapping rate, and the non-cleavable methylene-modified mRNA would serve as a control for specificity of the signal. Studies of this type could be conducted for either Dcp2 (using compound **3**) or DcpS (using compound **4**).

Experimental

General information

All intermediates were separated by ion-exchange chromatography on DEAE-Sephadex A-25 (HCO_3^- form) column using a linear gradient of triethylammonium bicarbonate (TEAB) buffer in deionised water and after evaporation under reduced pressure with addition of ethanol, isolated as triethylammonium (TEA) salts. Final products were purified by means of semi-preparative RP HPLC and after a three-times repeated freeze-drying procedure they were isolated as ammonium salts. Yields were calculated either based on sample weight or optical units of the product. In this study an optical unit is defined as the absorption of compound solution in 0.1 M phosphate buffer (pH = 6, or 7 if a compound does not contain 7-methylguanosine residue) at 260 nm multiplied by volume of the solution in cm^3. Analytical HPLC measurements were performed on an Agilent Tech. Series 1200 using a Supelcosil LC-18-T RP column (4.6 × 250 mm, flow rate 1.3 mL/min) with a 0–50% linear gradient of methanol in 0.05M ammonium acetate buffer (pH 5.9) for 15 min, UV-detection at 260 nm and fluorescence detection (excitation at 280 nm and detection at 337 nm). Semi-preparative HPLC preparations were performed on an Agilent Tech. Series 1200 apparatus using Discovery RP Amide C-16 HPLC column (25 cm × 21.2 mm, 5 μm, flow rate 5.0 mL/min) with a 0–30% linear gradient of acetonitrile in 0.05 M ammonium acetate buffer (pH 5.9) for 120 or 180 min, and UV-detection at 260 nm. The structure and homogeneity of each final product were confirmed by chromatography on RP HPLC, mass spectrometry using negative electrospray ionization (MS ESI-) and NMR spectroscopy. ^{1}H NMR and ^{31}P NMR spectra were recorded at 25 °C on a Varian UNITY-plus spectrometer at 399.94 MHz and 161.90 MHz respectively. ^{1}H NMR chemical shifts were reported to sodium 3-trimethylsilyl-[2,2,3,3-D4]-propionate (TSP) in D_2O as an internal reference and ^{31}P NMR chemical shifts were reported to 20% phosphorus acid in D_2O as an external reference. Mass spectra were recorded on a MicromassQToF 1 MS spectrometer.

General procedure for fluorescent tagging using isotoic or N-methylisotoic anhydrides

Synthesis of Mant or Ant-tagged nucleotides was achieved by following the synthesis procedure for Ant-GTP as reported by Hiratsuka [53] with modifications. A one equivalent of an appropriate nucleotide (TEA or sodium salt) was dissolved in MQ water and the pH was adjusted to 9.5 with 1M NaOH. To the solution, 0.2 eq of appropriate anhydride was added with continuous stirring. The pH of the solution was maintained at 9.6 by titration with NaOH and the anhydride was constantly added in small quantities (ca 0.2 eq) until the whole

amount of the substrate was converted to products. Completion of the reaction was achieved within 6–8 hours, next the pH of the solution was adjusted to 7.0 with 50% acetic acid and the reaction mixture was filtered through a syringe filter to obtain a clear solution.

Purification of fluorescent-tagged nucleotides by size-exclusion chromatography and conversion to sodium salts

The products were separated via size-exclusion chromatography on a G15 Sephadex column (GE Healtcare) using MQ water as a eluent and after evaporation under reduced pressure isolated as triethylammonium (TEA) salts. TEA salts were converted to sodium salt by precipitation with a solution of anhydrous $NaClO_4$ (2.5 eq. per negative charge) in dry acetone (~20 cm^3/1 cm^3 of MQ water). Afterwards the mixture was cooled at 4 °C, the precipitate was filtered, washed repeatedly with cold, dry acetone and dried *in vacuo* over P_4O_{10}.

Preparation of 2′-*O*-methylguanosine

2′-*O*-Methylguanosine was prepared as described previously by methylation of a 6-*O*-ethyl derivative of guanosine with diazomethane, which results in the formation of two regioisomers: 2′-*O*-methyl-6-*O*-ethylguanosine and 3′-methyl-6-*O*-ethylguanosine. Both compounds were separated by column chromatography using Dowex 1×2 Ion-Exchange Resin (200–400 mesh) using 0.3 M TEAB buffer as an eluent in an isocratic system.

General procedure for preparation of nucleotide imidazolide derivatives

All imidazolides were prepared according to previously described procedure[66]. An appropriate nucleotide (1 eq., TEA salt), imidazole (10 eq.) and 2,2′-dithiodipyridine (3 eq.) were dissolved in dimethylformamide (DMF) (the final concentration of nucleotide was ca 0.1 M). Triethylamine (2 eq.) and triphenylphosphine (3 eq.) were added subsequently and the mixture was stirred for 8–10 h. The product was precipitated from the reaction mixture with a solution of anhydrous $NaClO_4$ (2.5 eq. one negative charge) in dry acetone (~10 cm^3/1 cm^3 of DMF). Afterwards the mixture was cooled at 4 °C, the precipitate was filtered, washed repeatedly with cold, dry acetone and dried *in vacuo* over P_4O_{10}.

Coupling of imidazolidates with nucleotides

In each case coupling leads to elongation of polyphosphate chain by one phosphate unit. This process was accomplished by dissolving the corresponding imidazolide (~1.25 eq) with an appropriate TEA salt (1 eq) and anhydrous $ZnCl_2$ (8 eq.) in anhydrous DMF. After 1–2 hours the reaction was quenched *via* addition of solution of EDTA (1.25 mol per 1 mol of $ZnCl_2$) in a water solution of $NaHCO_3$. In the next step, the pH was adjusted to 7 and the product was purified *via* ion-exchange chromatography on DEAE–Sephadex.

Selective methylation at N7 position

7-methylguanosine was prepared by treatment of guanosine with $(CH_3O)_2SO_2$ in DMA according to previously reported procedure. All nucleoside mono- and diphosphates containing 7-methylguanosine residue were synthesised employing CH_3I in DMSO as was described earlier.

Phosphorylation and phosphonylation

2′-O-methylguanosine monophosphate was prepared by employing Yoshikawa reaction with distilled phosphorus oxychloride in trimethyl phosphate as a solvent, which has been described in previous studies[66]. Phosphonylation of guanosine with methylenebis-(phosphonic dichloride), resulting in $GpCH_2p$, was achieved *via* modified Yoshikawa procedure as described in the literature[7].

3′ (2′)-*O*-*N*-methylanthraniloyl guanosin-5′-yl monophosphate; 3′ (2′) Mant-GMP—GMP (TEA salt, 100 mg, 0.25 mmol) was dissolved in 5.5 cm^3 of MQ water and the synthesis was performed as described in the general procedure. 13.2 mg (TEA salt; 10% yield) of white solid was obtained.

3′ (2′)-*O*-*N*-methylanthraniloyl 7-methylguanosin-5′-yl monophosphate; 3′ (2′) Mant-m^7GMP; (9)

Method 1: m^7GMP (TEA salt, 160 mg, 0.333 mmol) was dissolved in 5.5 cm^3 of MQ water and the synthesis was performed as described in the general procedure. The product was purified employing ion-exchange chromatography on DEAE–Sephadex (TEAB gradient 0–1.2 M). 1520 optical units (TEA salt; yield 31%) of pale yellow solid were obtained.

Method 2: Purification by size-exclusion chromatography and conversion to sodium salt. Starting from 77 mg of m^7GMP and applying the same procedure as for Method 1 1.4 mg (sodium salt; yield 2%) of pale yellow solid was obtained.

isomer C2′ ^{1}H NMR (ppm): 8.04 (1H, m, H6), 7.55 (1H, m, H4), 6.87 (1H, m, H3), 6.77 (1H, m, Hz, H5), 6.36 (1H, d, $J_{H1'\text{-}H2'}$=4.2 Hz, $H1'_{m7G}$), 5.79 (1H, dd, $J_{H1'\text{-}H2'}$=4.2 Hz, $J_{H2'\text{-}H3'}$=5.0 Hz, $H2'_{m7G}$), 4.8 (1H, overlapped with HDO, $H3'_{m7G}$), 4.53 (1H, m, $H4'_{m7G}$), 4.16–4.04 (2H, m, $H5'_{m7G}$, $H5''_{m7G}$), 4.14 (3H, s, N-CH_{3m7G}), 2.87 (3H, s, N-CH_3). ^{31}P NMR (ppm): 3.87 (1P, s). ESI MS: calcd: 509.11911 Found: 509.12169.

isomer C3′ ^{1}H NMR (ppm): 8.10 (1H, m, H6), 8.04, 7.55 (1H, m, H4), 6.90 (1H, m, H3), 6.77 (1H, m, Hz, H5), 6.26 (1H, d, $J_{H1'\text{-}H2'}$=5.6 Hz, $H1'_{m7G}$), 5.65 (1H, dd, $J_{H2'\text{-}H3'}$=4.8 Hz, $J_{H3'\text{-}H4'}$=3.0 Hz, $H3'_{m7G}$), 5.02 (1H, dd, $J_{H1'\text{-}H2'}$=5.7 Hz, $J_{H2'\text{-}H3'}$=4.8 Hz, $H2'_{m7G}$), 4.71 (1H, m, $H4'_{m7G}$), 4.23–4.19 (1H, m, $H5'_{m7G}$), 4.14 (3H, s, N-CH_{3m7G}), 4.10–4.05 (1H, m, $H5''_{m7G}$), 2.91 (3H, s, N-CH_3). ^{31}P NMR (ppm): 3.87 (1P, s). ESI MS: calcd: 509.11911 Found: 509.12169.

^{31}P NMR (ppm): 3.87 (1P, s). ESI MS: calcd: 509.11911 Found: 509.12169.

3′ (2′)-*O*-*N*-methylanthraniloyl 7-methylguanosin-5′-yl diphosphate; 3′ (2′) Mant-m^7GDP; (7)

Method 1: m^7GDP (TEA salt, 100 mg, 0.137 mmol; purity 90%) was dissolved in 2.5 cm^3 of MQ water and the synthesis was performed as described in the general procedure. The product was purified employing ion-exchange chromatography on DEAE–Sephadex (TEAB gradient 0–1.2 M). 1900 optical units (TEA salt; yield 92%) of pale yellow solid were obtained.

Method 2: Purification by size-exclusion chromatography and conversion to sodium salt. Starting from 101 mg of m^7GDP and applying the same procedure as for Method 1. The product was purified employing ion-exchange chromatography on DEAE–Sephadex (TEAB gradient 0–1.2 M). 18.8 mg (sodium salt; yield 18%) of pale yellow solid was obtained.

isomer C2′ ^{1}H NMR (ppm): 8.04 (1H, m, H6), 7.54 (1H, m, H4); 6.87 (1H, m, H3), 6.74(1H, m, H5), 6.32 (1H, s, $J_{H1'\text{-}H2'}$=3.0 Hz, $H1'_{m7G}$), 5.78 (1H, dd, $J_{H1'\text{-}H2'}$=3.0 Hz, $J_{H2'\text{-}H3'}$=5.0 Hz, $H2'_{m7G}$), 4.87 (1H, dd, $J_{H2'\text{-}H3'}$=5.3 Hz, $J_{H3'\text{-}H4'}$=5.0 Hz, $H3'_{m7G}$), 4.51 (1H, m, $H4'_{m7G}$), 4.45–4.27 (2H, m, $H5''_{m7G}$, $H5'_{m7G}$), 4.12 (3H, s, N-$CH3_{m7G}$), 2.86 (3H, s, N-CH_3). ^{31}P NMR (ppm): −6.05 (1P, s, Pβ); −10.52 (1P, s,). ESI MS: calcd: 589.085466 Found: 589.08546.

isomer C3′ ^{1}H NMR (ppm): 8.09 (1H, m, H6), 7.54 (1H, m, H4), 6.87 (1H, m, H3), 6.74 (1H, m, H5), 6.24 (1H, d, $J_{H1'\text{-}H2'}$=5.9 Hz, $H1'_{m7G}$), 5.66 (1H, dd, $J_{H2'\text{-}H3'}$=5.4 Hz,

$J_{H3'\text{-}H4'}$=3.4 Hz, $H3'_{m7G}$), 5.07 (1H, dd, $J_{H1'\text{-}H2'}$=5.9 Hz, $J_{H2'\text{-}H3'}$=5.4 Hz, $H2'_{m7G}$), 4.73 (1H, m, $H4'_{m7G}$), 4.45–4.27 (2H, m, $H5''_{m7G}$, $H5'_{m7G}$), 4.14 (3H, s, N-$CH3_{m7G}$), 2.89 (3H, s, N-CH_3). ^{31}P NMR (ppm): −6.05 (1P, s, Pβ); −10.52 (1P, s,). ESI MS: calcd: 589.085466 Found: 589.08546.

3′ (2′)-*O*-*N*-methylanthraniloyl 7-methylguanosin-5′-yl 1,2 methylene-diphosphate; 3′ (2′) Mant-m^{7}GpCH$_2$p; (8)

Method 1: m^{7}GpCH$_2$p (TEA salt, 120 mg, 0.176 mmol) was dissolved in 3.0 cm^3 of MQ water and the synthesis was performed as described in the general procedure. 1400 optical units (TEA salt; yield 53%) of pale yellow solid were obtained.

Method 2: Purification by size-exclusion chromatography and conversion to sodium salt. Starting from 64 mg of m^{7}GpCH$_2$p TEA salt and applying the same procedure as for Method 1 6.6 mg (sodium salt; yield 10%) of pale yellow solid was obtained.

isomer C2′ ^{1}H NMR (ppm): 8.04 (1H, m, H6), 7.54 (1H, m, H4); 6.87(1H, m, H3), 6.74 (1H, m, H5), 6.32 (1H, d, $J_{H1'\text{-}H2'}$=3.0 Hz, $H1'_{m7G}$), 5.67 (1H, m, $H2'_{m7G}$), 4.84 (1H, m, $H3'_{m7G}$), 4.57 (1H, m, $H4'_{m7G}$), 4.36 (2H, m, $H5'_{m7G}$, $H5''_{m7G}$), 4.13 (3H, s, N-CH_{3m7G}), 2.86 (3H, s, N-CH_3), 2.22 (2H, d, P-CH_2-P) ^{31}P NMR (ppm): 22.44 (1P, s, Pα), 11.84 (1P, s, Pβ). ESI MS: calcd: 587.10620 Found: 587.10641.

isomer C3′ ^{1}H NMR (ppm): 8.10 (1H, m, H6), 7.54 (1H, m, H4); 6.87(1H, m, H3), 6.74 (1H, m, H5), 6.24 (1H, d, $J_{H1'\text{-}H2'}$=6.0 Hz, $H1'_{m7G}$), 5.51 (1H, m, $H3'_{m7G}$), 5.10 (1H, m, $H2'_{m7G}$(), 4.73 (1H, m, $H4'_{m7G}$), 4.36 (2H, m, $H5'_{m7G}$, $H5''_{m7G}$), 4.15 (3H, s, N-CH_{3m7G}), 2.89 (3H, s, N-CH_3), 2.22 (2H, d, P-CH_2-P). ^{31}P NMR (ppm): 22.44 (1P, s, Pα), 11.84 (1P, s, Pβ). ESI MS: calcd: 587.10620 Found: 587.10641.

3′ (2′)-*O*-anthraniloyl 7-methylguanosin-5′-yl diphosphate; 3′ (2′) Ant-m^{7}GDP; (6)

Method 1: m^{7}GDP (TEA salt, 250 mg, 0.378 mmol; purity 90%) was dissolved in 6.5 cm^3 of MQ water and the synthesis was performed as described in the general procedure. The product was purified employing ion-exchange chromatography on DEAE–Sephadex (TEAB gradient 0–1.2 M). 1304 optical units (TEA salt; yield 26%) of pale yellow solid were obtained.

Method 2: Purification by size-exclusion chromatography and conversion to sodium salt. Starting from 101 mg of m^{7}GDP and applying the same procedure as for Method 1 12.4 mg (sodium salt; yield 11%) of pale yellow solid was obtained.

isomer C2′ ^{1}H NMR (ppm): 8.01 (1H, m, H6), 7.42 (1H, m, H4), 6.86 (1H, m, H3), 6.82 (1H, m, H5), 6.36 (1H, m, $J_{H1'\text{-}H2'}$=1.8 Hz, $H1'_{m7G}$), 5.84 (1H, m, $H2'_{m7G}$), 4.90 (1H, dd, $J_{H2'\text{-}H3'}$=6.2 Hz, $J_{H3'\text{-}H4'}$=5.5 Hz, $H3'_{m7G}$), 4.42 (1H, m, $H4'_{m7G}$), 4.47–4.26 (2H, m, $H5''_{m7G}$, $H5'_{m7G}$), 4.14 (3H, s, N-CH_{3m7G}). ^{31}P NMR (ppm): −6.31 (1P, d, $J_{P\beta\text{-}P\alpha}$=23.0 Hz, Pβ), −10.76 (1P, d, $J_{P\beta\text{-}P\alpha}$=23.0 Hz, Pα). ESI MS: calcd: 575.06982 Found:575.07000.

isomer C3′ ^{1}H NMR (ppm): 8.04 (1H, m, H6), 7.42 (1H, m, H4), 6.86 (1H, m, H3), 6.82 (1H, m, H5), 6.25 (1H, d, $J_{H1'\text{-}H2'}$=5.6 Hz, $H1'_{m7G}$), 5.67 (1H, m, $H3'_{m7G}$), 5.09 (1H, dd, $J_{H1'\text{-}H2'}$=5.6 Hz, $J_{H2'\text{-}H3'}$=5.2 Hz, $H2'_{m7G}$), 4.52 (1H, m, $H4'_{m7G}$), 4.47–4.26 (2H, m, $H5''_{m7G}$, $H5'_{m7G}$), 4.16 (3H, s, N-CH_{3m7G}). ^{31}P NMR (ppm): −6.31 (1P, d, $J_{P\beta\text{-}P\alpha}$=23.0 Hz, Pβ), −10.76 (1P, d, $J_{P\beta\text{-}P\alpha}$=23.0 Hz, Pα). ESI MS: calcd: 575.06982 Found:575.07000.

2′-*O*-methyl, 3′-*O*-anthraniloyl 7-methylguanosin-5′-yl monophosphate; Ant-$m_2^{7,2'-O}$GMP; (10)

Method 1: $m^{7,2'-O}$GMP (TEA salt, 100 mg, 0.2 mmol) was dissolved in 4 cm^3 of MQ water and synthesis was performed as described in the general procedure. The product was purified employing ion-exchange chromatography on DEAE–Sephadex (TEAB gradient 0–0.9 M). 630 optical units (TEA salt; yield 21%) of pale yellow solid were obtained.

Method 2: Purification by size-exclusion chromatography and conversion to sodium salt. Starting from 77 mg of $m^{7,2'-O}$GMP and applying the same procedure as for Method 1. 26.7 mg (sodium salt; yield 11%) of pale yellow solid was obtained.

^{1}H NMR (ppm): 7.86 (1H, m, H6), 7.37 (1H, m, H4), 6.81(1H, m, H3), 6.68 (1H, m, H5), 6.27 (1H, d, $J_{H1'-H2'}$=5.5 Hz, H1′), 5.74 (1H, dd, $J_{H2'-H3'}$=4.9 Hz, $J_{H3'-H4'}$=2.7 Hz, H3′), 4.75 (1H, dd, $J_{H1'-H2'}$=5.5 Hz, $J_{H2'-H3'}$=4.9 Hz, H2′), 4.71 (1H, m, H4′), 4.20–4.08 (2H, m, H5′, H5″), 4.08 (3H, s, N-CH_3), 3.51 (3H, s, O-CH_3). ^{31}P NMR (ppm): 3.56 (1P, s). ESI MS: calcd: 509.11911 Found: 509.12169.

guanosin-5′-yl diphosphate; GDP; (19)—TEA phosphate (440 mg; 2.3 mmol) and anhydrous zinc chloride (750 mg 5.75 mmol) were stirred in 2 cm^3 of anhydrous DMF until both substrates dissolved. Subsequently GMP-Im (Na salt, 490 mg, 1.15 mmol; purity 85%) and anhydrous zinc chloride (750 mg 5.75 mmol) were dissolved in 2cm^3 of DMF. Both solutions were mixed and TEA (0.125 cm^3; 1.71 mmol) was added to the mixture. The reaction was performed for 20 h and quenched by addition of EDTA (825 mg; 2.21 mmol) dissolved in 50 cm^3 of 0.5 M $NaHCO_3$ solution. The product was purified employing ion-exchange chromatography on DEAE-Sephadex (TEAB gradient 0–1.0 M). 7480 optical units (TEA salt; yield 65%) were obtained.

7-methylguanosin-5′-yl diphosphate; m^7GDP; (11)—GDP (TEA salt, 395 mg; 0.62 mmol) was dissolved in 6 cm^3 of anhydrous DMSO and CH_3I (0.6 cm^3; 9.3 mmol) was added. The reaction was performed 2 for hours and quenched by addition of 75 cm^3 of MQ water. The pH was adjusted to 7.0 using solid $NaHCO_3$ and the product was purified employing ion-exchange chromatography on DEAE-Sephadex (TEAB gradient 0–0.9 M). 3890 optical unis of white solid were obtained (TEA salt; yield 53%).

7-methylguanosin-5′-yl monophosphate; m^7GMP; (12)—GMP (TEA salt, 500 mg; 1.08 mmol) was dissolved in 12.5 cm^3 of anhydrous DMSO and CH_3I (0.6 cm^3; 9.3 mmol) was added. The reaction was performed 3 for hours and quenched by addition of 150 cm^3 of MQ water. The pH was adjusted to 7.0 using solid $NaHCO_3$ and the product was purified employing ion-exchange chromatography on DEAE-Sephadex (TEAB gradient 0–0.7 M). 4935 optical unis of white solid were obtained (TEA salt; yield 40%).

2′-*O*-methylguanosin-5′-yl monophosphate; $m^{2'-O}$GMP—2′-*O*-mG (1000 mg; 3.4 mmol) was suspended in 20 cm^3 of trimethyl phosphate and the reaction flask was cooled in ice to 0°C. To a cold suspension $POCl_3$ (0.638 cm, 6.8 mol,) was added, the reaction was performed for 2 hours and it was quenched *via* addition of 200 cm^3 of MQ water. The pH was adjusted to 7.0 using $NaHCO_3$ and the product was separated *via* ion-exchange chromatography (TEAB gradient 0–0.7 M). 1330 mg (TEA salt; yield 74%) of a white solid were obtained.

7,2′-*O*-dimethylguanosin-5′-yl monophosphate; $m_2^{7,2'-O}$GMP; (14)—$m^{2'-O}$GMP (TEA salt, 500 mg; 1.08 mmol) was dissolved in 12 cm^3 of anhydrous DMSO and CH_3I (0.6 cm^3; 9.5 mmol) was added. The reaction was performed for 3 hours and quenched by

addition of 150 cm^3 of MQ water. The pH was adjusted to 7.0 using solid $NaHCO_3$ and the product was purified employing ion-exchange chromatography on DEAE-Sephadex (TEAB gradient 0–0.7 M). 8500 optical unis of white solid were obtained (TEA salt; yield 70%).

guanosin-5′-yl 1,2 methylene-diphosphate; GpCH$_2$p; (20)—Guanosine (250 mg, 0.883 mmol) was dissolved in 10 cm^3 of trimethyl phosphate and cooled to 0 °C on an ice bath and methylenebis(phosphonic dichloride) (665 mg, 3.532 mmol) was added to the stirred mixture. The reaction was performed at 0 °C and after 90 minutes it was quenched by addition of 100 cm^3 of MQ water, then solid $NaHCO_3$ was added untill pH = 7. The product was purified *via* ion–exchange chromatography on DEAE-Sephadex (TEAB gradient 0–1.0 M). 7115 optical units of white solid were obtained (TEA salt; yield 67%).

7-methylguanosin-5′-yl 1,2 methylene-diphosphate; m^{7}GpCH$_2$p; (13)—GpCH$_2$p (TEA salt, 250 mg; 0.389 mmol) was dissolved in 4.2 cm^3 of anhydrous DMSO and CH_3I (0.2 cm^3; 3.112 mmol) was added. The reaction was performed for 3 hours and quenched by addition of 50 cm^3 of MQ water. The pH was adjusted to 7.0 using solid $NaHCO_3$ and the product was purified employing ion-exchange chromatography on on DEAE-Sephadex (TEAB gradient 0–1.0 M). 2260 optical units of white solid were obtained (TEA salt; yield 51%).

guanosin-5′-yl monophosphate P-imidazolide; GMP-Im/Na$^+$; (15)—Starting from GMP (TEA salt; 250 mg; 0.54 mmol) 221 mg of white solid was obtained (TEA salt; yield 95%).

1P-guanosin-5′-yl diphosphate P2-imidazolide; GDP-Im/Na+; (17)—Starting from GDP (TEA salt; 300 mg; 0.467 mmol) 250 mg of white solid was obtained (yield 98%).

1P-guanosin-5′-yl 1,2 methylene-diphosphate P2-imidazolide; GpCH$_2$p-Im/Na$^+$; (18)—Starting from GpCH$_2$p (TEA salt; 150 mg; 0.234 mmol) 118 mg of white solid was obtained (TEA salt; yield 95%).

P1-(3′ (2′)-*O*-anthraniloyl-7-methylguanosin-5′-yl) P3-guanosin-5′-yl triphosphate; 3′ (2′)Ant-m^{7}GpppG; (1)—Ant-m^{7}GDP (TEA salt, 60 mg; 0.077 mmol), GMP-Im (sodium salt; 48 mg 0.115 mmol) and anhydrous $ZnCl_2$ (125 mg, 0.93 mmol) were dissolved in anhydrous DMF. After 70 minutes the reaction was quenched *via* addition of solution of EDTA (400 mg, 1.19 mmol) in a water solution of $NaHCO_3$ (200 mg, 2.38 mmol). In next step the pH was adjusted to 7 and the product was purified employing ion-exchange chromatography on DEAE–Sephadex (TEAB gradient 0–1.4 M). 760 optical units (yield 39%) of pale yellow solid were obtained. The product was purified on HPLC yielding 25.4 mg (NH_4 salt; yield 34%).

isomer C2′ ^{1}H NMR (ppm): 9.13 (1H, s, $H8_{m7G}$), 7.99 (1H, s, $H8_G$), 7.86 (1H, m, H6); 7.36 (1H, m, H4), 6.76 (1H, m, H3), 6.70 (1H, m, H5), 6.18(1H, d, $J_{H1'-H2'}$=3.0 Hz, $H1'_{m7G}$), 5.78 (1H, d, $J_{H1'-H2'}$=5.5 Hz, $H1'_G$), 5.72 (1H, dd, $J_{H1-H2'}$=3.0 Hz, $J_{H2'-H3'}$=4.5 Hz, $H2'_{m7G}$), 4.75 (1H, m, overlapped with HDO, $H3'_{m7G}$), 4.61 (1H, dd, $J_{H1'-H2'}$=5.5, $J_{H2'-H3'}$=5.2, $H2'_G$), 4.50–4.21 (6H, m, $H4'_G$, $H4'_{m7G}$, $H5'_G$, H''_G, $H5'_{m7G}$, $H5''_{m7G}$), 4.47 (1H, dd, $J_{H2'-H3'}$=5.2, $J_{H3'-H4'}$=2.1 $H3'_G$), 4.07 (3H, s, N-CH_3) ^{31}P NMR (ppm): −10.59 (2P, m, $J_{P\beta-P\alpha(P\gamma)}$=19.5 Hz, Pα, Pγ), −22.26 (1P, d, $J_{P\beta-P\alpha(P\gamma)}$=19.5 Hz, Pβ). ESI MS: calcd: 920.11725 Found: 920.11565.

isomer C3′ ^{1}H NMR (ppm): 9.21 (1H, s, $H8_{m7G}$), 7.99 (1H, s, $H8_G$), 7.86 (1H, m, H6), 7.36 (1H, m, H4), 6.80 (1H, m, H3), 6.70 (1H, m, H5), 6.10 (1H, d, $J_{H1'-H2'}$=6.0 Hz, $H1'_{m7G}$), 5.78 (1H, d, $J_{H1'-H2'}$=5.5 Hz, $H1'_G$), 5.51 (1H, dd, $J_{H2'-H3'}$=5.1 Hz, $J_{H3'-H4'}$=2.8 Hz,

$H3'_{m7G}$), 4.97 (1H, dd, $J_{H1'-H2'}$ =6.0 Hz, $J_{H2'-H3'}$=5.1 Hz, $H2'_{m7G}$), 4.66 (1H, m, $H4'_{m7G}$), 4.61 (1H, dd, $J_{H1'-H2'}$=5.5, $J_{H2'-H3'}$=5.2, $H2'_G$), 4.50–4.21 (6H, m, $H4'_G$, $H4'_{m7G(A)}$, $H5'_G$, H ″$_G$, $H5'_{m7G}$, $H5''_{m7G}$), 4.47 (1H, dd, $J_{H2'-H3'}$=5.2, $J_{H3'-H4'}$=2.1 $H3'_G$), 4.09 (3H, s, N-CH_3). ^{31}P NMR (ppm): −10.59 (2P, m, $J_{P\beta-P\alpha(P\gamma)}$=19.5 Hz, Pα, Pγ), −22.26 (1P, d, $J_{P\beta-P\alpha(P\gamma)}$=19.5 Hz, Pβ). ESI MS: calcd: 920.11725 Found: 920.11565.

P1-(2′-*O*-methyl-3′-*O*-anthraniloyl-7-methylguanosin-5′-yl) P3-guanosin-5′-yl triphosphate; Ant-m$_2^{7,2'-O}$GpppG; (5)—Ant-m$_2^{7,2'-O}$GMP (TEA salt, 32 mg; 0.06 mmol) and GDP-Im (sodium salt; 39 mg 0.072 mmol) and anhydrous $ZnCl_2$ (90 mg, 0.67 mmol) were dissolved in 0.5 cm^3 anhydrous DMF. After 90 minutes the reaction was quenched *via* addition of a solution of EDTA (185 mg, 0.55 mmol) in water solution of $NaHCO_3$ (92 mg, 1.1 mmol). In the next step the pH was adjusted to 7 and the product was purified employing ion-exchange chromatography on DEAE–Sephadex (TEAB gradient 0–1.4 M). 1250 optical units (yield 83%) of pale yellow solid were obtained. The product was purified on HPLC yielding 15.4 mg (NH_4 salt; yield 26%).

^{1}H NMR (ppm): 9.20 (1H, s, $H8_{m7G}$), 8.03 (1H, s, $H8_G$), 7.84 (1H, m, H6), 7.38 (1H, m, H4), 6.81 (1H, m, H3), 6.71 (1H, m, H5), 6.10 (1H, d, $J_{H1'-H2')}$=5.5 Hz, $H1'_{m7G}$), 5.78 (1H, d, $J_{H1'-H2'}$=5.5 Hz, $H1'_G$), 5.60 (1H, t, $J_{H2'-H3'}$=$J_{H3'-H4'}$=3.2 Hz, $H2'_{m7G}$), 4.66 (2H, m, $H2'_{m7G}$, $H4'_{m7G}$), 4.61 (1H, t, $J_{H1'-H2'}$=5.5 $J_{H2'-H3'}$=5.0 Hz, $H2'_G$), 4.45 (1H, dd, $J_{H2'-H3'}$=5.0, $J_{H3'-H4'}$=3.4, $H3'_G$), 4.42 (1H, s, $H4'_G$), 4.30 (4H, m, $H5'_{m7G}$, $H5''_{m7G}$, $H5'_G$, $H5''_G$), 4.10 (3H, s, N-CH_3), 3.47 (3H, s, O-CH_3). ^{31}P NMR (ppm): −10.60 (2P, d, $J_{P\beta-P\alpha(P\gamma)}$=18.5 Hz, Pα, Pγ,), −22.19 (1P, d, $J_{P\beta-P\alpha(P\gamma)}$=18.5 Hz Pβ,). ESI MS: calcd: 934.1329 Found: 934.13275.

P1-(3′ (2′)-*O*-*N*-methylanthraniloyl-7-methylguanosin-5′-yl) P3-guanosin-5′-yl triphosphate; 3′ (2′)Mant-m^{7}GpppG; (2)—Mant-m^{7}GDP (TEA salt, 90 mg; 0.115 mmol), GMP-Im (sodium salt; 70 mg 0.168 mmol) and anhydrous $ZnCl_2$ (180 mg, 1.34 mmol) were dissolved in anhydrous DMF. After 70 minutes the reaction was quenched *via* addition of a solution of EDTA (560 mg, 1.5 mmol) in a water solution of $NaHCO_3$ (252 mg, 3 mmol). In the next step the pH was adjusted to 7 and the product was purified employing ion-exchange chromatography on DEAE–Sephadex (TEAB gradient 0–1.4 M). 1070 optical units (yield 36%) of pale yellow solid were obtained. The product was purified on HPLC yielding 19.4 mg (NH_4 salt; yield 17%).

isomer C2′ ^{1}H NMR (ppm): 9.12 (1H, s, $H8_{m7G}$), 7.98 (1H, s, $H8_G$), 7.87 (1H, m, H6), 7.42 (1H, m, H4), 6.68 (1H, m, H3), 6.61 (1H, m, H5), 6.16 (1H, d, $J_{H1'-H2'}$=2.7 Hz, $H1'_{m7G}$), 5.77 (1H, d, $J_{H1'-H2'}$=4.2, $H1'_G$), 5.65 (1H, m, $H2'_{m7G}$), 4.65 (1H, m, $H2'_G$), 4.58 (1H, dd, $J_{H2'-H3'}$=5.2, $J_{H3'-H4'}$=5.0 Hz, $H3'_{m7G}$), 4.51 (1H, m, $H4'_{m7G}$), 4.42–4.20 (5H, m, $H4'_G$, $H5''_{m7G}$, $H5'_{m7G}$, $H5''_G$, $H5'_G$), 4.05 (3H, s, N-CH_3), 2.74 (3H, s, N-CH_3). ^{31}P NMR (ppm): −14.44 (2P, d, $J_{P\beta-P\alpha(P\gamma)}$=19.1 Hz, Pα, Pγ), −26.00 (1P, d, $J_{P\beta-P\alpha(P\gamma)}$=19.1 Hz, Pβ). ESI MS: calcd: 934.1329 Found: 934.13313.

isomer C3′ ^{1}H NMR (ppm): 9.17 (1H, s, $H8_{m7G}$), 7.98 (1H, s, $H8_G$), 7.81 (1H, m, H6), 7.42 (1H, m, H4), 6.68 (1H, m, H3), 6.53 (1H, m, H5), 6.10 (1H, d, $J_{H1'-H2'}$=5.7 Hz, $H1'_{m7G}$), 5.77 (1H, d, $J_{H1'-H2'}$=4.2, $H1'_G$), 5.49 (1H, m, $H3'_{m7G}$), 4.98 (1H, dd, $J_{H1'-H2'}$=5.7 Hz, $J_{H2'-H3'}$=5.2 Hz, $H2'_{m7G}$), 4.65 (1H, m, $H2'_G$), 4.47 (2H, m, $H3'_G$, $H4'_{m7G}$), 4.42–4.20 (5H, m, $H4'_G$, $H5''_{m7G}$, $H5'_{m7G}$, $H5''_G$, $H5'_G$), 4.05 (3H, s, N-CH_3), 2.82 (3H, s, N-CH_3). ^{31}P NMR (ppm): −14.44 (2P, d, $J_{P\beta-P\alpha(P\gamma)}$=19.1 Hz, Pα, Pγ), −26.00 (1P, d, $J_{P\beta-P\alpha(P\gamma)}$=19.1 Hz, Pβ). ESI MS: calcd: 934.1329 Found: 934.13313.

P1-(3′ (2′)-*O*-*N*-methylanthraniloyl-7-methylguanosin-5′-yl) P3-guanosin-5′-yl 1–2 methylenetriphosphate; 3′ (2′)Mant-m^{7}GpCH$_2$ppG; (4)—Mant-m^{7}GpCH$_2$p

(TEA salt, 59 mg; 0.075 mmol), GMP-Im (Na salt; 39 mg 0.075 mmol) and anhydrous $ZnCl_2$ (80 mg, 0.6 mmol) were dissolved in anhydrous DMF. After 4 hours the reaction was quenched *via* addition of solution of EDTA (240 mg, 0.63 mmol) in a water solution of $NaHCO_3$ (110 mg, 1.33 mmol). In the next step the pH was adjusted to 7 and the product was purified employing ion-exchange chromatography on DEAE–Sephadex (TEAB gradient 0–1.4 M). 460 optical units (yield 23%) of pale yellow solid were obtained. The product was purified on HPLC yielding 6.3 mg (NH_4 salt; yield 8%).

isomer C2′ ^{1}H NMR (ppm): 9.41 (1H, s, $H8_{m7G}$), 8.00 (1H, s, $H8_G$), 7.93 (1H, m, H6), 7.47 (1H, m, H4), 6.99 (1H, m, H3), 6.93 (1H, m, H5), 6.22 (1H, m, $H1'_{m7G}$), 5.78 (1H, m, $H1'_G$), 5.67 (1H, m, $H2'_{m7G}$), 4.67 (1H, m, overlapped with HDO, $H3'_{m7G}$), 4.62 (1H, m, $H2'_G$), 4.52 (1H, m, $H4'_{m7G}$), 4.48 (1H, m, $H3'_G$), 4.39–4.20 (5H, m, $H4'_G$, $H5''_{m7G}$, $H5'_{m7G}$, $H5''_G$, $H5'_G$), 4.05 (3H, s, N-$CH_{3(m7G)}$), 2.74 (3H, s, N-CH3), 2.42 (2H, m, P-CH_2-P). ^{31}P NMR (ppm): 18.31 (1P, m, Pβ), 8.04 (1P, s. Pγ), −10.09 (1P, s, Pα). ESI MS: calcd: 932.15363 Found: 932.15324.

isomer C3′ 9.49 (1H, s, $H8_{m7G}$), 8.02 (1H, s, $H8_G$), 7.93 (1H, m, H6), 7.47 (1H, m, H4), 6.76 (1H, m, H5), 6.67 (1H, m, H3), 6.14 (1H, m, $H1'_{m7G}$), 5.78 (1H, m, $H1'_G$), 5.55 (1H, m, $H3'_{m7G}$), 5.07 (1H, m, $H2'_{m7G}$), 4.92 (1H, m, overlapped with HDO, $H3'_{m7G}$), 4.62 (1H, m, $H2'_G$), 4.52 (1H, m, $H4'_{m7G}$), 4.48 (1H, m, $H3'_G$), 4.39–4.20 (5H, m, $H4'_G$, $H5''_{m7G}$, $H5'_{m7G}$), $H5''_G$, $H5'_G$), 4.05 (3H, s, N-$CH_{3(m7G)}$), 2.82 (3H, s, N-CH_3), 2.42 (2H, m, P-CH_2-P). ^{31}P NMR (ppm): 18.31 (1P, m, Pβ), 8.04 (1P, s. Pγ), −10.09 (1P, s, Pα). ESI MS: calcd: 932.15363 Found: 932.15324.

P1-(3′ (2′)-*O*-*N*-methylanthraniloyl-7-methylguanosin-5′-yl) P3-guanosin-5′-yl 2–3 methylenetriphosphate; 3′ (2′)Mant-m^{7}GppCH$_2$pG; (3)—Mant-m^{7}GMP (TEA salt, 49 mg; 0.08 mmol), $GpCH_2p$-Im (Na salt; 50 mg 0.08 mmol) and anhydrous $ZnCl_2$ (110 mg, 0.8 mmol) were dissolved in anhydrous DMF. After 10 hours the reaction was quenched *via* addition of solution of EDTA (330 mg, 0.9 mmol) in a water solution of $NaHCO_3$ (150 mg, 1.8 mmol). In the next step the pH was adjusted to 7 and the product was purified employing ion-exchange chromatography on DEAE–Sephadex (TEAB gradient 0–1.4 M). 675 optical units (yield 36%) of pale yellow solid were obtained. The product was purified on HPLC yielding 8.8 mg (NH_4 salt; yield 12% (partially decomposed during lyophilisation).

isomer C2′ ^{1}H NMR (ppm): 9.20 (1H, s, $H8_{m7G}$), 8.01 (1H, s, $H8_{(G)}$), 7.89 (1H, m, H6), 7.44 (1H, m, H4), 6.70 (1H, m, H3), 6.61 (1H, m, H5), 6.18 (1H, d, $J_{H1'-H2'}$=3.5 Hz, $H1'_{m7G}$)), 5.72 (1H, d, $J_{H1'-H2'}$=4.7 Hz, $H1'_G$), 5.64 (1H, dd, $J_{H2'-H3'}$=5.2 Hz, $J_{H2'-H3'}$=3.5 Hz, $H2'_{m7G}$), 4.68 (1H, overlapped with HDO, $H3'_{m7G}$) 4.62 (1H, dd, $H2'_G$), $J_{H1'-H2'}$=5.2 Hz, $J_{H2'-H3'}$=4.5 Hz), 4.45 (1H, t, $J_{H2'-H3'}$=$J_{H3'-H4'}$=4.5 Hz, $H3'_G$), 4.40–4.16 (6H, m, $H4'_G$, $H4'_{m7G}$, $H5''_{m7G}$, $H5'_{m7G}$, $H5'_G$, $H5''_G$), 4.06 (3H, s, N-$CH_{3(m7G)}$), 2.73 (3H, s, N-CH_3), 2.38 (2H, m, P-CH_2-P, J_{CH2-P} = 20.5 Hz). ^{31}P NMR (ppm): 18.05 (1P, m, Pβ), 8.36 (1P, m. Pγ), −10.18 (1P, m, Pα). ESI MS: calcd: 932.15363. Found: 932.15313.

isomer C3′ ^{1}H NMR (ppm): 9.24 (1H, s, $H8_{m7G,}$), 8.01 (1H, s, $H8_{(G)}$), 7.89 (1H, m, H6), 7.44 (1H, m, H4), 6.70 (1H, m, H3), 6.61 (1H, m, H5), 6.10 (1H, d, $J_{H1'-H2'}$=5.9 Hz, $H1'_{m7G}$), 5.74 (1H, d, $J_{H1-H2'}$=5.2 Hz, $H1'_G$), 5.48 (1H, dd, $J_{H2'-H3'}$=4.7 Hz, $J_{H3'-H4'}$=2.7 Hz, $H3'_{m7G}$), 4.97 (1H, dd, $J_{H1'-H2'}$=5.9 Hz, $J_{H2'-H3'}$=4.7 Hz, $H2'_{m7G}$), 4.62 (1H, dd, $H2'_{(G)}$, $J_{H1'-H2'}$=5.2 Hz, $J_{H2'-H3'}$=4.5 Hz), 4.49 (1H, s, $H4'_{m7G}$), 4.45 (1H, t, $J_{H2'-H3'}$=$J_{H3'-H4'}$=4.5 Hz, $H3'_G$), 4.40–4.16 (6H, m, $H4'_G$, $H5''_{m7G}$, $H5'_{m7G}$, $H5'_G$, $H5''_G$), 4.06 (3H, s, N-$CH_{3(m7G)}$), 2.79 (3H, s, N-CH_3), 2.38 (2H, m, P-CH_2-P, J_{CH2-P} = 20.5 Hz). ^{31}P NMR (ppm): 18.05 (1P, m, Pβ), 8.36 (1P, m. Pγ), −10.18 (1P, m, Pα). ESI MS: calcd: 932.15363. Found: 932.15313.

Spectroscopic measurements

General information—Methyl anthranilate (AntOMe) and methyl ***N***-methylanthranilate (MantOMe) were purchased from Sigma–Aldrich and used without further purification. All the solvents used were also purchased from Sigma–Aldrich and were either HPLC grade or the highest grade available. Water was deionized using a Simplicity 185 system produced by Millipore. The pH of solutions was adjusted with a phosphate buffer (PBS) (0.067 M) and confirmed using a JENWAY 3030 pH Meter calibrated with standard buffers. Typically 10 buffer solutions ranging from pH 5 to 9 were employed. Absorption spectra were recorded on a Cary 5000 UV-Vis-NIR Spectrophotometer (Varian Inc.) using 1 cm square quartz cuvettes. The entire spectra from 220 to 450 nm (in 0.5 nm steps) were employed to calculate the pKa values and the spectra of the individual ionic forms according to the previously used method[67]. Fluorescence emission spectra were recorded using a Cary Eclipse spectrofluorometer (Varian Inc.), the cell-housing block of which was thermostated to 25 °C within 0.1 °C. The emission and excitation spectra of the samples were measured in a 1 cm × 0.4 cm cuvette at 25°C. The fluorescence spectra of the samples were measured using a suitable excitation wavelength and emission range in order to calculate the total area under the curve. Quantum yields were determined by comparing the integral intensity of the steady state emission spectra excited at a long-wave maximum of absorption (corrected for the refractive index of the solvent and absorbance) with quinine sulphate in 0.1 M sulphuric acid, using a quantum yield (QY) of 0.57[67]. The optical density of the samples at this excitation wavelength did not exceed 0.1. For the photostability study, time-based fluorescence steady-state measurements were acquired with the excitation slit opened to maximum.

Fluorescence lifetime measurements—For fluorescence lifetime measurements samples were excited at 340 nm. The excitation source was a PLS-340 sub-nanosecond pulsed LED (340 nm, optical pulse duration: 410 ps FWHM) driven by a PDL800-D driver. Intensity decays were collected by a time-domain technique using a FluoTime 200 lifetime fluorometer (PicoQuant, GmbH) equipped with an R3809U-50 microchannel plate photomultiplier (MCP-PMT, Hamamatsu), and a PicoHarp300 TCSPC module. Polarizers were set to magic angle conditions and the fluorescence was observed through a 100 mm focal length single grating emission monochromator (ScienceTech 9030). All the samples were prepared directly before measurements and the recordings were taken at a temperature of 20°C. The fluorescence lifetimes were calculated using the FluoFit software package (version 4.4). All fluorescence decay curves were fitted using a single exponential function. The analysis involved iterative reconvolution fitting of a sum of exponentials to the experimentally recorded decays:

$$I(t) = \sum \alpha_i \exp(-t/\tau_i) \quad (1)$$

where $I(t)$ is the intensity at time t, α_i is the amplitude of a single exponential component i, and τ_i is the lifetime of the component.

Biological assays employing eIF4E and DcpS—Human eIF4E[68] and human DcpS[69] were prepared as described previously. The protein concentrations were determined spectrophotometrically (ε_{280} = 52940 M^{-1} cm^{-1} and 30400 for eIF4E and DcpS, respectively). Fluorescence measurements were run on an LS-50B spectrofluorometer (Perkin-Elmer Co., Hellma, Germany) in a quartz semi-micro cuvette with optical lengths of 4 and 10 mm for absorption and emission, respectively. Mant-m^7GpppG titrations were performed in 50 mM Hepes/KOH (pH 7.2), 100 mM KCl, 0.5 mM EDTA, and 1 mM DTT at 20 °C by adding appropriate aliquots of the eIF4E solutions to 100 nM Mant-m^7GpppG or MantOMe solution. DcpS-based kinetic assays were performed in 50 mM Tris/HCl, 200

mM KCl, 0.5 mM EDTA and 1 mM DTT (pH 7.2) at 20 °C. The reactions were initiated by addition of either 200 nM or 20 nM DcpS. Samples were excited at 260 nm and 361 nm and the fluorescence intensity was recorded at 360 and 446 nm when the substrate was m^7GpppG or Mant-m^7GpppG, respectively.

In vitro synthesis of RNAs

Capped RNAs were synthesised by *in vitro* transcription of plasmid pluc-A60 digested with *Nco*I, which yielded a capped RNA corresponding to the first 48 nt of firefly luciferase mRNA. All ribonucleotides were obtained in the presence of given cap analogues and 10 uCi/ul [α32-P] GTP (PerkinElmer) as described previously[12]. Reaction mixtures were extracted with phenol and chloroform; RNAs were separated from small-molecule impurities with NucAway spin columns (Ambion). The concentrations of RNAs were determined *via* measuring Cerenkov radiation in a scintillation counter (Beckman).

Decapping assays

His-tagged-GB-SpDcp1 and SpDcp2 were coexpressed in BL21(DE3)pLysS *Escherichia coli* cells from p-His-GB1 plasmids, which were generously donated by John Gross, UCSF. The enzymes were expressed and purified as described previously[70]. Capped 32P-labled oligonucleotides were subjected to digestion with GST-SpDcp1/2 at 37°C for 30 minutes in 50 mM Tris-Cl (pH 8 at 25°C), 50 mM NH_4Cl, 0.01% NP-40, 1 mM DTT and 5 mM $MgCl_2$. Reactions were quenched by adding two volumes of Precipitation/Inactivation Buffer III (Ambion). RNAs were precipitated at −20°C overnight, collected by centrifugation at 13000 g at 4°C for 20 min, purified by washing in 70% ethanol and collected again by centrifugation at 9000 g at 4 °C for 5 min. The quantity of RNA in the precipitated samples was determined *via* measurement of Cerenkov radiation in a scintillation counter (Beckman). The samples were resuspended in Sequencing Gel Loading Buffer (Ambion) and denatured at 95°C for 5 min. RNA sequencing gels (10% polyacrylamide) were run at 45–70 W for 3.5 h on a Base Runner Nucleic Acid Sequencer apparatus (International Biotechnologies). Gels were fixed in 5% acetic acid, 5% methanol for 10–15 min, dried onto Whatman 3MM filter paper (Fisher Scientific), and exposed to Blue X-ray film (Kodak). The intensity of individual bands was quantified by analyzing scanned film using the QuantityOne program (BioRad).

Translation efficiency in RRL of luciferase mRNA capped *in vitro*

Capped and polyadenylated luciferase mRNAs synthesised by *in vitro* transcription of a dsDNA template which contained: SP6 promoter sequence of DNA-dependent RNA polymerase, 5′UTR sequence of rabbit β-globin, the entire firefly luciferase ORF and a string of 31 adenosines. The *in vitro* transcription reaction mixture (40 ml) contained: SP6 transcription buffer (Fermentas), 0.7 mg of DNA template, 1 U/ml RiboLock Ribonuclease Inhibitor (Fermentas), 0.5 mM ATP/CTP/UTP and 0.1 mM GTP and 0.5 mM dinucleotide cap analogue (molar ratio cap analog:GTP 5:1). The reaction mixture was preincubated at 37 °C for 5 minutes before addition of SP6 RNA polymerase (Fermentas) to a final concentration of 1 U/ml and the reaction was continued for 45 minutes at 37 °C. After incubation, reaction mixtures were treated with DNase RQ1 (Promega), in transcription buffer, for 20 min at 37 °C at a concentration of 1U per 1 mg of DNA template. RNA transcripts were purified using NucAway Spin Columns (Ambion), the integrity of transcripts was checked on a non-denaturating 1% agarose gel and concentrations were determined *via* UV spectroscopy. A translation reaction in RRL was performed in 10 ml volume for 60 minutes at 30 °C, in conditions determined for cap dependent translation. The reaction mixture contained: 40% RRL lysate, mixture of amino acids (0.01 mM), $MgCl_2$ (1.2 mM), potassium acetate (170mM) and 5′-capped mRNA. Four different concentrations of each analyzed transcript were tested in the translation reaction. The activity of

synthesized luciferase was measured in a luminometer and the obtained data were processed using Origin 8 software (OriginLab).

Supplementary Material

Refer to Web version on PubMed Central for supplementary material.

Acknowledgments

The authors are grateful to the Laboratory of Biological NMR (Institute of Biochemistry and Biophysics, Polish Academy of Sciences, IBB PAS) for access to the NMR apparatus; Joanna Kowalska for critical reading of the manuscript, valuable comments and discussion; Jacek Oledzki from the Laboratory of Mass Spectrometry (IBB PAS) for recording MS spectra; John D. Gross from the University of California, San Francisco for Dcp1 and Dcp2 plasmid, Joanna Zuberek for valuable discussion and gift of eIF4E sample and Malgorzata Zytek for help with recording emission spectra. This study was supported by the Polish Ministry of Science and Higher Education (N N204 089438, N N301 096339), National Science Centre, Poland (UMO-2012/05/E/ST5/03893), a grant R01GM20818 from the National Institutes of Health (U.S.A), and a scholarship from the Foundation for Polish Science International Ph.D. Projects Program and the EU European Regional Development Fund (M.Z.).

Notes and references

1. Furuichi Y, Shatkin AJ. Adv Virus Res. 2000; 55:135–184. [PubMed: 11050942]
2. Jemielity J, Kowalska J, Rydzik AM, Darzynkiewicz E. New Journal of Chemistry. 2010; 34:829–844.
3. Westman B, Beeren L, Grudzien E, Stepinski J, Worch R, Zuberek J, Jemielity J, Stolarski R, Darzynkiewicz E, Rhoads RE, Preiss T. Rna-a Publication of the Rna Society. 2005; 11:1505–1513.
4. Konarska MM, Padgett RA, Sharp PA. Cell. 1984; 38:731–736. [PubMed: 6567484]
5. Contreras R, Gheysen D, Knowland J, van de Voorde A, Fiers W. Nature. 1982; 300:500–505. [PubMed: 6292733]
6. Stepinski J, Waddell C, Stolarski R, Darzynkiewicz E, Rhoads RE. RNA. 2001; 7:1486–1495. [PubMed: 11680853]
7. Kalek M, Jemielity J, Darzynkiewicz ZM, Bojarska E, Stepinski J, Stolarski R, Davis RE, Darzynkiewicz E. Bioorg Med Chem. 2006; 14:3223–3230. [PubMed: 16431118]
8. Grudzien-Nogalska E, Jemielity J, Kowalska J, Darzynkiewicz E, Rhoads RE. Rna-a Publication of the Rna Society. 2007; 13:1745–1755.
9. Kowalska J, Lewdorowicz M, Zuberek J, Grudzien-Nogalska E, Bojarska E, Stepinski J, Rhoads RE, Darzynkiewicz E, Davis RE, Jemielity J. Rna-a Publication of the Rna Society. 2008; 14:1119–1131.
10. Kowalska J, Lukaszewicz M, Zuberek J, Darzynkiewicz E, Jemielity J. Chembiochem. 2009; 10:2469–2473. [PubMed: 19739194]
11. Kuhn AN, Diken M, Kreiter S, Selmi A, Kowalska J, Jemielity J, Darzynkiewicz E, Huber C, Tureci O, Sahin U. Gene Therapy. 2010; 17:961–971. [PubMed: 20410931]
12. Su W, Slepenkov S, Grudzien-Nogalska E, Kowalska J, Kulis M, Zuberek J, Lukaszewicz M, Darzynkiewicz E, Jemielity J, Rhoads RE. Rna-a Publication of the Rna Society. 2011; 17:978–988.
13. Rydzik AM, Kulis M, Lukaszewicz M, Kowalska J, Zuberek J, Darzynkiewicz ZM, Darzynkiewicz E, Jemielity J. Bioorganic & Medicinal Chemistry. 2012; 20:1699–1710. [PubMed: 22316555]
14. Haran G. Curr Opin Struc Biol. 2012; 22:14–20.
15. Zhao R, Rueda D. Methods. 2009; 49:112–117. [PubMed: 19409995]
16. Flors C, Earnshaw WC. Curr Opin Chem Biol. 2011; 15:838–844. [PubMed: 22098720]
17. Leung BO, Chou KC. Appl Spectrosc. 2011; 65:967–980. [PubMed: 21929850]
18. Henriques R, Griffiths C, Hesper Rego E, Mhlanga MM. Biopolymers. 2011; 95:322–331. [PubMed: 21254001]

19. Sahoo H. Journal of Photochemistry and Photobiology C: Photochemistry Reviews. 2011; 12:20–30.
20. Truong K, Ikura M. Curr Opin Struc Biol. 2001; 11:573–578.
21. Ha T, Tinnefeld P. Annual Review of Physical Chemistry. 2012; 63:595–617.
22. Weiss S. Science. 1999; 283:1676–1683. [PubMed: 10073925]
23. Pareek CS, Smoczynski R, Tretyn A. J Appl Genet. 2011; 52:413–435. [PubMed: 21698376]
24. El-Sagheer AH, Brown T. Chem Soc Rev. 2010; 39:1388–1405. [PubMed: 20309492]
25. Sinkeldam RW, Greco NJ, Tor Y. Chemical reviews. 2010; 110:2579–2619. [PubMed: 20205430]
26. Toseland CP, Webb MR. Methods. 2010; 51:259–268. [PubMed: 20167273]
27. Hiratsuka T, Katoh T. J Biol Chem. 2003; 278:31891–31894. [PubMed: 12805386]
28. Okamoto A. Chem Soc Rev. 2011; 40:5815–5828. [PubMed: 21660343]
29. Ostergaard ME, Hrdlicka PJ. Chem Soc Rev. 2011; 40:5771–5788. [PubMed: 21487621]
30. Hiratsuka T. European Journal of Biochemistry. 2003; 270:3479–3485. [PubMed: 12919312]
31. Khan MA, Goss DJ. Biochemistry. 2005; 44:4510–4516. [PubMed: 15766281]
32. Bagshaw C. Journal of cell science. 2001; 114:459–460. [PubMed: 11171313]
33. Jameson DM, Eccleston JF. Fluorescence Spectroscopy. 1997; 278:363–390.
34. Geduhn J, Dove S, Shen YQ, Tang WJ, Konig B, Seifert R. Journal of Pharmacology and Experimental Therapeutics. 2011; 336:104–115. [PubMed: 20962032]
35. Suryanarayana S, Wang JL, Richter M, Shen YQ, Tang WJ, Lushington GH, Seifert R. Biochemical Pharmacology. 2009; 78:224–230. [PubMed: 19492438]
36. Goettle M, Dove S, Steindel P, Shen Y, Tang WJ, Geduhn J, Koenig B, Seifert R. Molecular Pharmacology. 2007; 72:526–535. [PubMed: 17553924]
37. Shen Y, Lee YS, Soelaiman S, Bergson P, Lu D, Chen A, Beckingham K, Grabarek Z, Mrksich M, Tang WJ. EMBO J. 2002; 21:6721–6732. [PubMed: 12485993]
38. Gille A, Guo J, Mou TC, Doughty MB, Lushington GH, Seifert R. Biochem Pharmacol. 2005; 71:89–97. [PubMed: 16271707]
39. Pinto C, Lushington GH, Richter M, Gille A, Geduhn J, Konig B, Mou TC, Sprang SR, Seifert R. Biochemical Pharmacology. 2011; 82:358–370. [PubMed: 21620805]
40. Mou TC, Gille A, Fancy DA, Seifert R, Sprang SR. J Biol Chem. 2005; 280:7253–7261. [PubMed: 15591060]
41. Emmrich T, El-Tayeb A, Taha H, Seifert R, Müller CE, Link A. Bioorganic & Medicinal Chemistry Letters. 2010; 20:232–235. [PubMed: 19914832]
42. Wei CC, Balasta ML, Ren J, Goss DJ. Biochemistry. 1998; 37:1910–1916. [PubMed: 9485317]
43. Ren JH, Goss DJ. Nucleic Acids Research. 1996; 24:3629–3634. [PubMed: 8836193]
44. Zdanowicz A, Thermann R, Kowalska J, Jemielity J, Duncan K, Preiss T, Darzynkiewicz E, Hentze MW. Molecular Cell. 2009; 35:881–888. [PubMed: 19782035]
45. Deshmukh MV, Jones BN, Quang-Dang DU, Flinders J, Floor SN, Kim C, Jemielity J, Kalek M, Darzynkiewicz E, Gross JD. Molecular Cell. 2008; 29:324–336. [PubMed: 18280238]
46. Mathonnet G, Fabian MR, Svitkin YV, Parsyan A, Huck L, Murata T, Biffo S, Merrick WC, Darzynkiewicz E, Pillai RS, Filipowicz W, Duchaine TF, Sonenberg N. Science. 2007; 317:1764–1767. [PubMed: 17656684]
47. Grudzien E, Kalek M, Jemielity J, Darzynkiewicz E, Rhoads RE. J Biol Chem. 2006; 281:1857–1867. [PubMed: 16257956]
48. Kalek M, Jemielity J, Grudzien E, Zuberek J, Bojarska E, Cohen LS, Stepinski J, Stolarski R, Davis RE, Rhoads RE, Darzynkiewicz E. Nucleosides Nucleotides Nucleic Acids. 2005; 24:615–621. [PubMed: 16247999]
49. Nawrot B, Sprinzl M. Nucleos Nucleot. 1998; 17:815–829.
50. Nawrot B, Milius W, Ejchart A, Limmer S, Sprinzl M. Nucleic acids research. 1997; 25:948–954. [PubMed: 9023103]
51. Wright M, Miller AD. Bioorg Med Chem Lett. 2004; 14:2813–2816. [PubMed: 15125938]
52. Hiratsuka T. J Biol Chem. 1982; 257:13354–13358. [PubMed: 6292187]

53. Kadokura M, Wada T, Urashima C, Sekine M. Tetrahedron Letters. 1997; 38:8359–8362.
54. Kalek M, Jemielity J, Stepinski J, Stolarski R, Darzynkiewicz E. Tetrahedron Letters. 2005; 46:2417–2421.
55. Raut S, Heck A, Vishwanatha J, Sarkar P, Mody A, Luchowski R, Gryczynski Z, Gryczynski I. J Photochem Photobiol B. 2011; 102:241–245. [PubMed: 21237671]
56. Beeby A, Jones AE. J Photochem Photobiol B. 2001; 64:109–116. [PubMed: 11744397]
57. Turchiello RF, Lamy-Freund MT, Hirata IY, Juliano L, Ito AS. Biophysical chemistry. 1998; 73:217–225. [PubMed: 17029728]
58. Davies DB, Danyluk SS. Biochemistry. 1974; 13:4417–4434. [PubMed: 4414857]
59. Altona C, Sundaralingam M. J Am Chem Soc. 1972; 94:8205–8212. [PubMed: 5079964]
60. Jemielity J, Lukaszewicz M, Kowalska J, Czarnecki J, Zuberek J, Darzynkiewicz E. Org Biomol Chem. 2012; 10:8570–8574. [PubMed: 22832840]
61. Liu H, Rodgers ND, Jiao X, Kiledjian M. EMBO J. 2002; 21:4699–4708. [PubMed: 12198172]
62. Singh J, Salcius M, Liu SW, Staker BL, Mishra R, Thurmond J, Michaud G, Mattoon DR, Printen J, Christensen J, Bjornsson JM, Pollok BA, Kiledjian M, Stewart L, Jarecki J, Gurney ME. ACS Chem Biol. 2008; 3:711–722. [PubMed: 18839960]
63. Wypijewska A, Bojarska E, Stepinski J, Jankowska-Anyszka M, Jemielity J, Davis RE, Darzynkiewicz E. FEBS J. 2010; 277:3003–3013. [PubMed: 20546305]
64. Sonenberg, Hinnebusch AG. Cell. 2009; 136:731–745. [PubMed: 19239892]
65. Ziemniak M, Strenkowska M, Kowalska J, Jemielity J. Future Med Chem. 2013; 5:1141–1172. [PubMed: 23795970]
66. Stepinski J, Bretner M, Jankowska M, Felczak K, Stolarski R, Wieczorek Z, Cai AL, Rhoads RE, Temeriusz A, Haber D, Darzynkiewicz E. Nucleos Nucleot. 1995; 14:717–721.
67. Wieczorek Z, Stepinski J, Jankowska M, Lonnberg H. J Photochem Photobiol B. 1995; 28:57–63. [PubMed: 7791006]
68. Zuberek J, Jemielity J, Jablonowska A, Stepinski J, Dadlez M, Stolarski R, Darzynkiewicz E. Biochemistry. 2004; 43:5370–5379. [PubMed: 15122903]
69. Wypijewska A, Bojarska E, Lukaszewicz M, Stepinski J, Jemielity J, Davis RE, Darzynkiewicz E. Biochemistry. 2012; 51:8003–8013. [PubMed: 22985415]
70. Floor SN, Jones BN, Hernandez GA, Gross JD. Nat Struct Mol Biol. 2010; 17:1096–1101. [PubMed: 20711189]

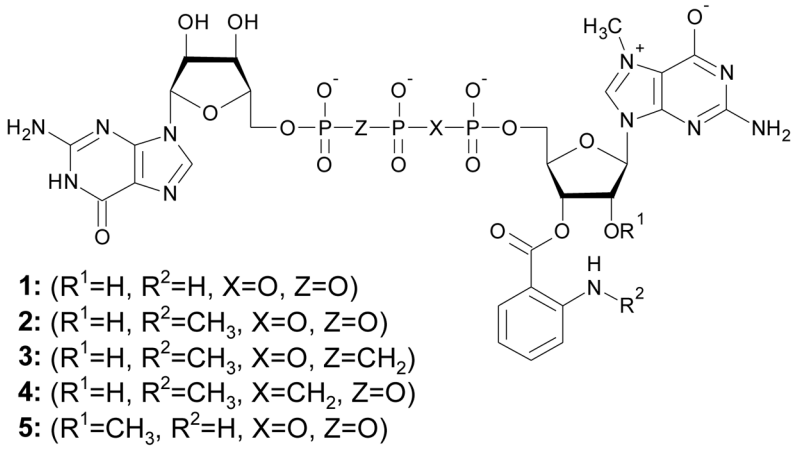

Fig. 1.
Structures of synthesised cap analogues

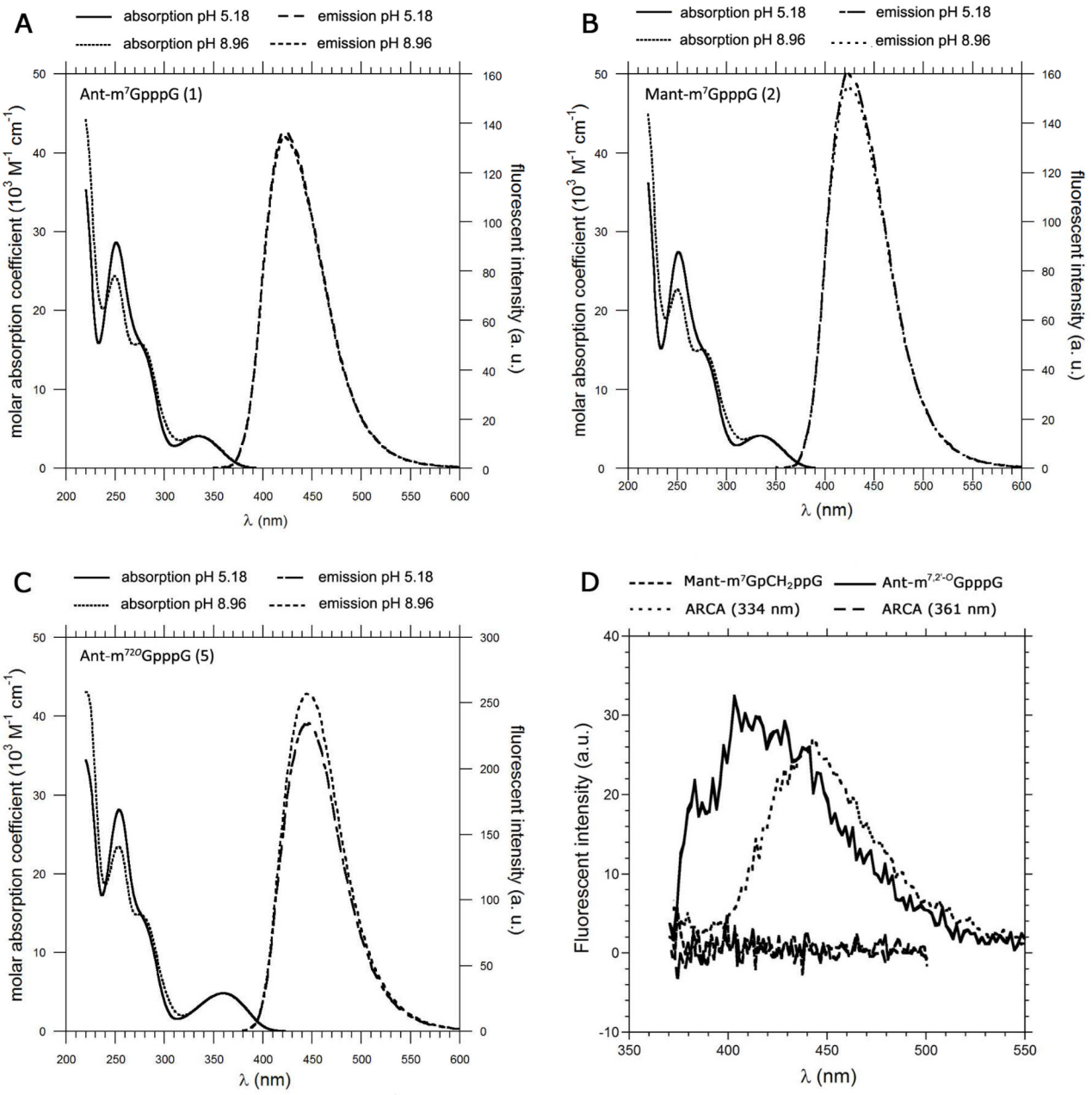

Fig. 2.

Absorbance and emission spectra of Ant-m^{7}GpppG (A), Mant-m^{7}GpppG (B), and Ant-$m_2^{7,2'O}$GpppG (C) in phosphate buffer at pH 5.18 and pH 8.96. Emission spectra of the indicated fluorescent mRNAs containing either Ant- or Mant-modified caps (D). The concentration of each cap analogue was 11.7 μM. The concentrations of RNA were 6.7 nM and 10.4 nM for Ant-or Mant-labelled transcripts, respectively. The concentration of ARCA-capped RNA was 10 nM.

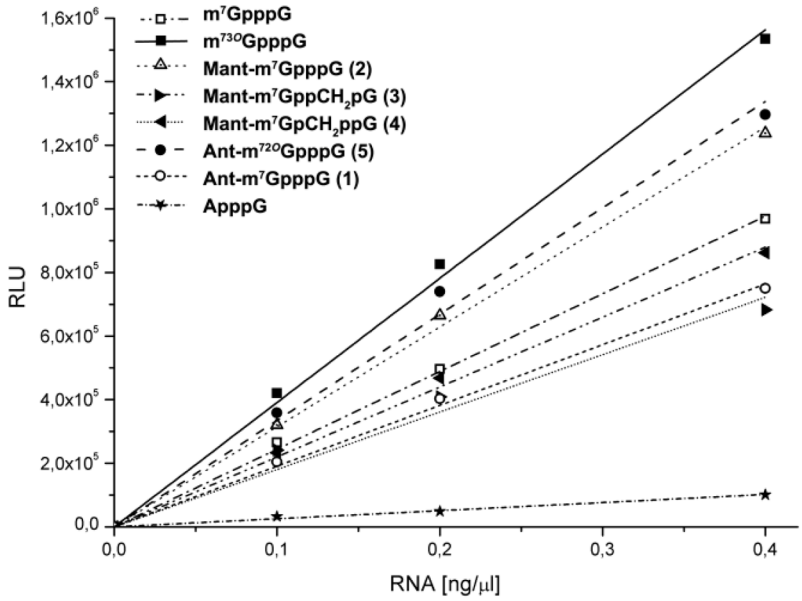

Fig. 3.
Luciferase activity as a function of concentration of mRNA capped with various ARCAs.

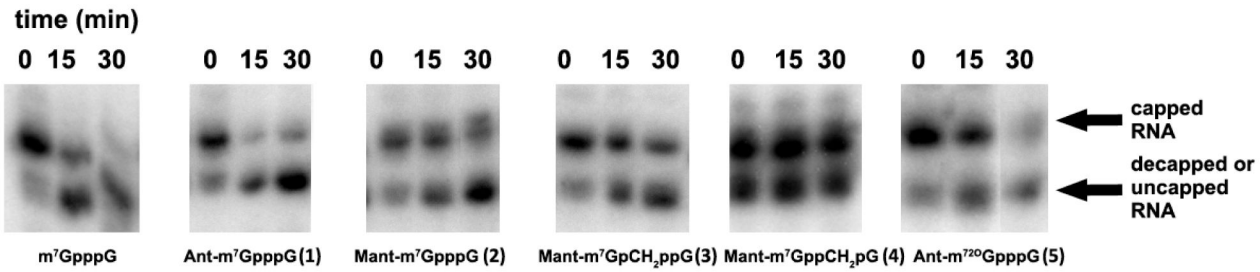

Fig. 4.

In vitro hydrolysis of capped oligonucleotides by SpDcp1/2. All transcripts were synthesized from an Nco1-cut pluc-A60 template with T7 polymerase in the presence of [α-^{32}P]GTP and various cap dinucleotides. After treatment with SpDcp1/2 for the indicated times, samples were loaded on a 10% RNA sequencing gel as described in Materials and Methods.

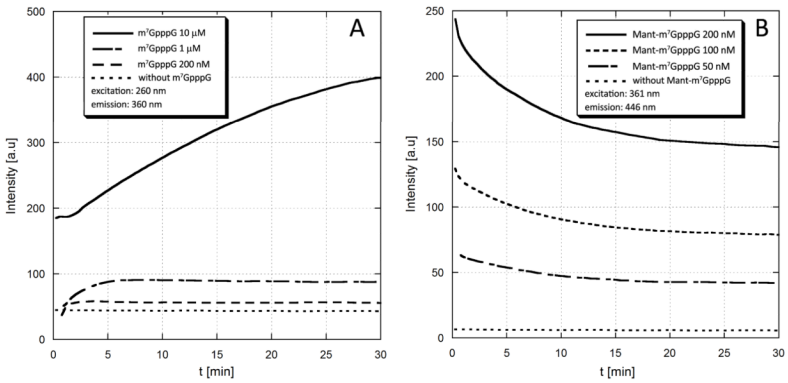

Fig. 5.

Monitoring the DcpS-catalyzed enzymatic hydrolysis of unlabeled (m^7GpppG) and Mant-labeled (Mant-m^7GpppG) cap analogues by spectrofluorymetry. (A). Unlabeled m^7GpppG is cleaved by DcpS to m^7GMP and GDP. The fluorescence intensity of the sample observed at the wavelength characteristic for m^7G moiety (ex.=260 nm, em.=360 nm) increases along with reaction progress because in the dinucleotide (m^7GpppG) fluorescence of m^7G is partially quenched by intramolecular stacking between m^7G and G. The fluorescence changes were sufficient to monitor reaction progress at concentration of 1 μM or higher(B) Mant-m^7GpppG (**2**) is cleaved by DcpS to Mant-m^7GMP and GDP. The fluorescence intensity of the sample observed at the wavelength characteristic for Mant moiety (ex.=361 nm, em.=446 nm) decreases along with reaction progress because the fluorescence of Mant in dinucleotide is enhanced by intramolecular interactions with hydrophobic parts of the second nucleoside (guanosine). The fluorescence changes were sufficient to monitor reaction progress at concentration of 50 nM or higher, i.e. 20-fold lower than for unlabeled m^7GpppG. The DcpS concentration was 20 nM (experiment with m^7Gp_3G) or 200 nM (experiment with Mant-m^7GpppG).

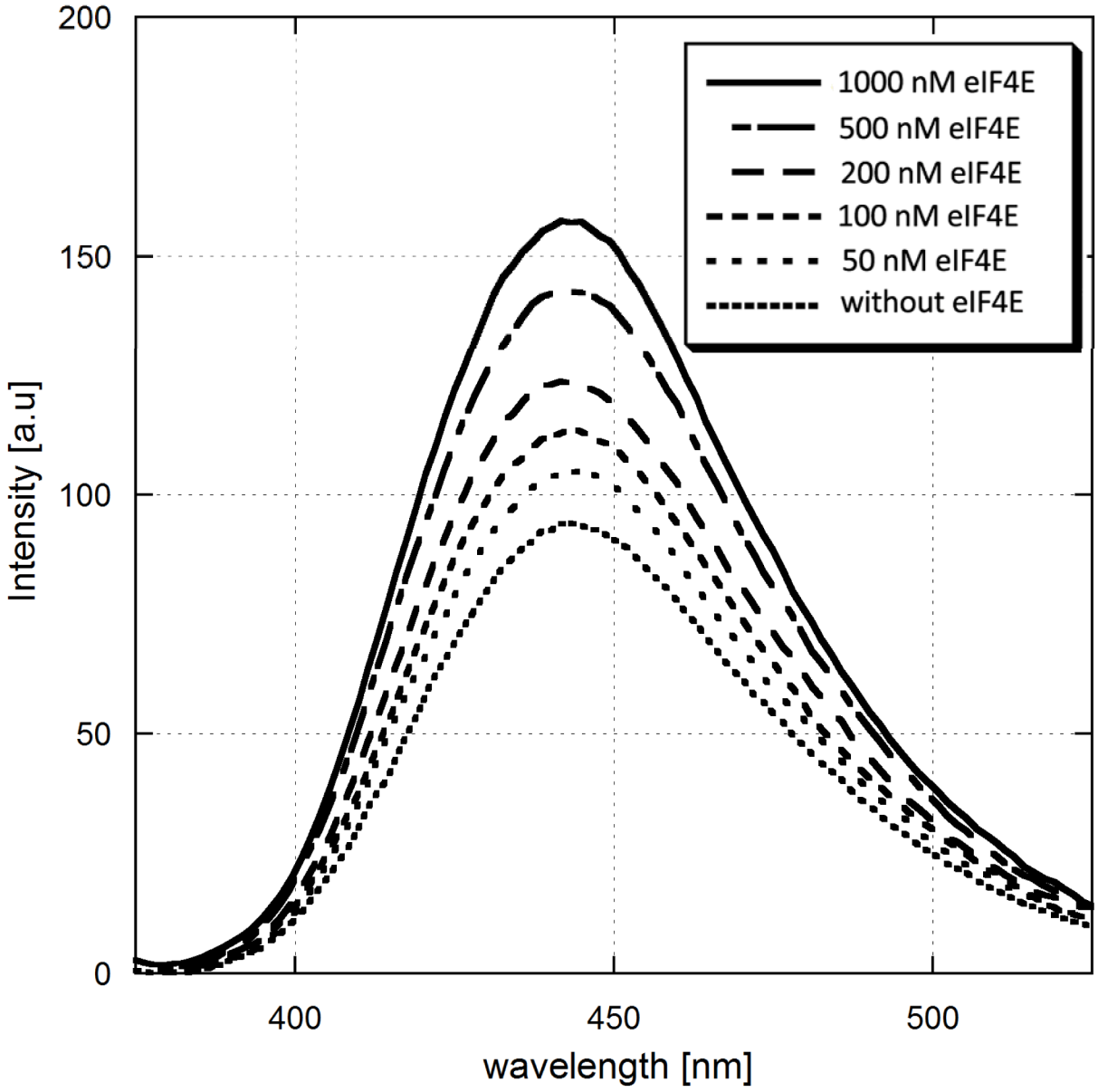

Fig. 6.

Sensitivity of Mant –labeled cap analog 2 to changes in local polarity caused by protein binding. Increase in Mant-m7GpppG fluorescence intensity observed upon addition of increasing amounts of eIF4E protein. The concentration of Mant-m7GpppG was 200 nM and the eIF4E concentrations were in range 50–1000 nM.

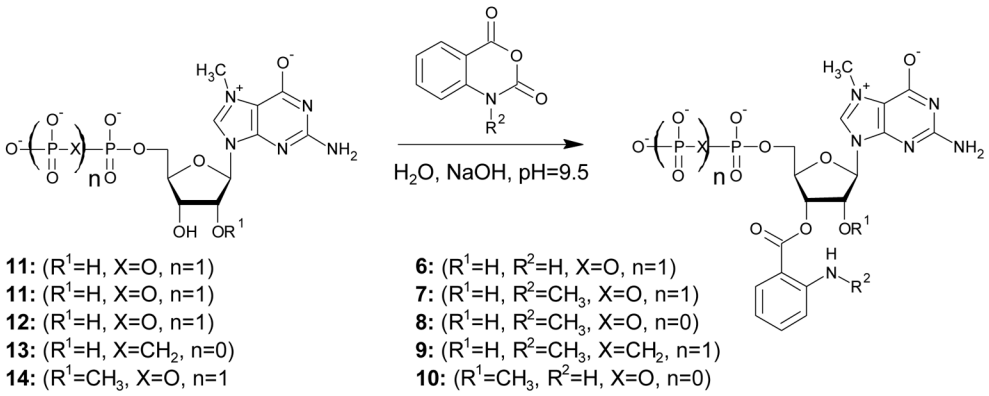

11: (R^1=H, X=O, n=1)
11: (R^1=H, X=O, n=1)
12: (R^1=H, X=O, n=1)
13: (R^1=H, X=CH_2, n=0)
14: (R^1=CH_3, X=O, n=1

6: (R^1=H, R^2=H, X=O, n=1)
7: (R^1=H, R^2=CH_3, X=O, n=1)
8: (R^1=H, R^2=CH_3, X=O, n=0)
9: (R^1=H, R^2=CH_3, X=CH_2, n=1)
10: (R^1=CH_3, R^2=H, X=O, n=0)

Scheme 1.
Labelling of m^7G-containing nucleotides with isatoic or N-methylisatoic anhydride. For the sake of clarity only 3′ regioisomer of compounds **6**-**9** is depicted.

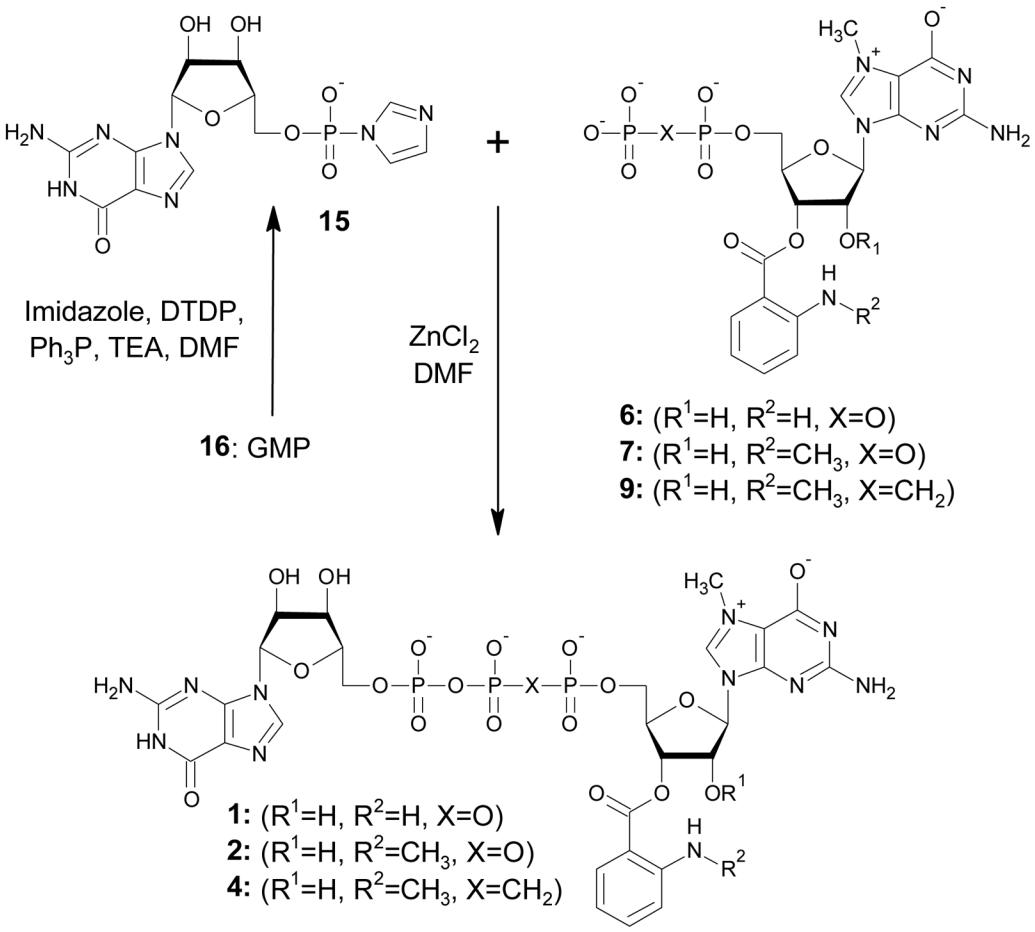

Scheme 2.

Synthesis of **1**, **2**, **4**. DTDP – 2;2′-dithiodipyridine; Ph3P – triphenylphosphine; TEA – triethylamine; DMF - dimethylformamid

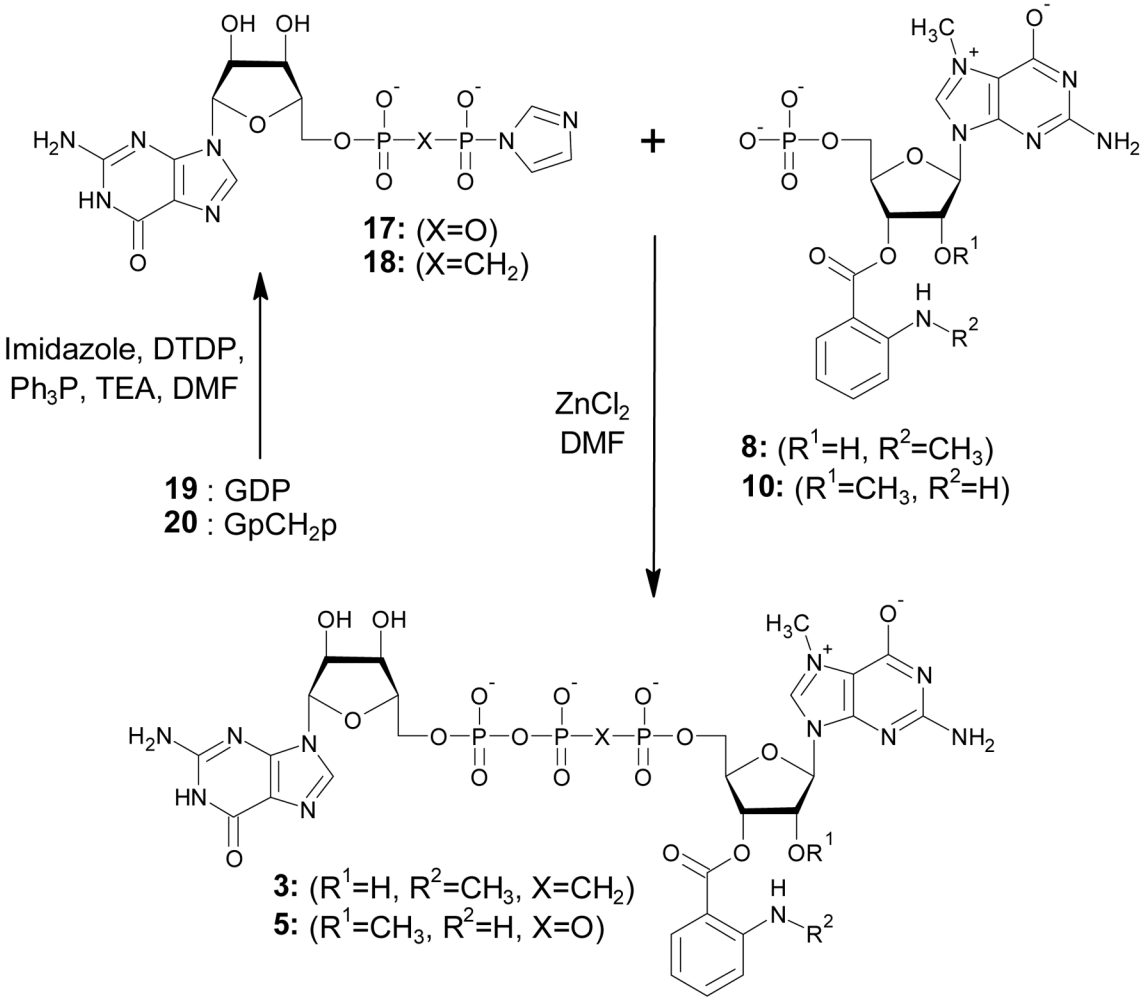

Scheme 3.

Synthesis of **3**, **5.** DTDP – 2;2′-dithiodipyridine; Ph_3P – triphenylphosphine; TEA – triethylamine; DMF - dimethylformamid

Table 1

Reactants and products structures and yields of formation dinucleotide cap analogues.

Product (No)	$\varepsilon_{\lambda 260}$ ($M^{-1}cm^{-1}$)	Nucleophile (No)	Activated nucleotide (No)	HPLC conv. [%]	Yield [a/b] [%]
Ant-m^{7}GpppG (**1**)	21700	Ant-m^{7}GDP (**6**)	GMP-Im (**15**)	92	39/34
Mant-m^{7}GpppG (**2**)	26800	Mant-m^{7}GDP (**7**)	GMP-Im (**15**)	81	36/17
Mant-m^{7}GppCH$_2$pG (**3**)	26400	Mant-m^{7}GMP (**8**)	GpCH$_2$p-Im (**18**)	63	36/12
Mant-m^{7}GpCH$_2$ppG (**4**)	24000	Mant-m^{7}GpCH$_2$p (**9**)	GMP-Im (**15**)	72	23/8
Ant-m$_2^{7,2'\text{-}O}$GpppG (**5**)	21600	Ant-m$_2^{7,2'\text{-}O}$GMP (**10**)	GDP-Im (**17**)	95	83/26

[a] yield after ion exchange chromatography;

[b] yield after additional RP HPLC purification

Table 2

Spectroscopic properties of cap analogues in phosphate buffer and organic solvents.

Compound	Solution[a]	Absorption		Fluorescence		
		λ_{max} (nm)	$\varepsilon_{\lambda max}$ ($M^{-1}cm^{-1}$)	λ_{max} (nm)	QY	lifetime
Ant-m^{7}GpppG (**1**)	PBS pH = 5.18	334	4080	422.5	0.138	τ_1= 4.24 ns α_1= 0.3181 τ_2= 1.78 ns α_2= 0.6819 τ_{AV}= 2.56 ns χ_R^2=1.026
	PBS pH = 8.96	334	4040	422.5	0.135	τ_1= 4.15 ns α_1= 0.3172 τ_2= 1.79 ns α_2= 0.6828 τ_{AV}= 2.54 ns χ_R^2= 0.973
	MeOH	341.5	4800	415	0.453	τ_1= 7.30 ns α_1= 0.8493 τ_2= 3.20 ns α_2= 0.1507 τ_{AV}= 6.69 ns χ_R^2= 0.983
	EtOH	342.5	4670	413	0.594	τ_1= 8.08 ns χ_R^2= 1.195
Ant-m$^{7,2'\text{-}O}$GpppG (**5**)	PBS pH = 5.18	334	4110	424	0.161	τ_1= 4.23 ns α_1= 0,3689 τ_2= 2.04 ns α_2= 0.6311 τ_{AV}= 2.85 ns χ_R^2= 0.981
	PBS pH = 8.96	334	4100	424	0.156	τ_1= 4.23 ns α_1= 0.3903 τ_2= 2.10 ns α_2= 0.6097 τ_{AV}= 2.93 ns χ_R^2=0.954
Mant-m^{7}GpppG (**2**)	PBS pH = 5.18	361	4670	446	0.236	τ_1= 7.11 ns α_1= 0.4050 τ_2= 2.61 ns α_2= 0.5950 τ_{AV}= 4.43 ns χ_R^2= 1.101
	PBS pH = 8.96	361	4730	446	0.258	τ_1= 7.65 ns α_1= 0.4498 τ_2= 2.81 ns α_2= 0.5502 τ_{AV}= 4.99 ns χ_R^2= 1.084
	MeOH	358.5	5880	430	0.439	τ_1= 8.05 ns α_1= 0.6996 τ_2= 5.54 ns α_2= 0.3004 τ_{AV}= 7.30 ns χ_R^2= 1.036
	EtOH	358.5	5500	430	0.484	τ_1= 8.24 ns χ_R^2= 1.219

[a]PBS = phosphate buffer 0.067 M

Table 3

In vitro biochemical properties of cap analogues 1–5

No	Cap analogue	Capping efficiency [%]	*In vitro* decapping [%]		Translational efficiency[a]
			15 min	30 min	
1	Ant-m^{7}GpppG	50±3	26±8	44±16	0.82±0.27
2	Mant-m^{7}GpppG	57±2	37±11	52±12	1.34±0.05
3	Mant-m^{7}GppCH$_2$pG	63±5	5±9	11±10	0.69±0.11
4	Mant-m^{7}GpCH$_2$ppG	70±2	34±4	54±5	0.85±0.12
5	Ant-m$_2^{7,2'\text{-}O}$GpppG	68±6	29±9	48±9	1.26±0.28
-	m$_2^{7,3'\text{-}O}$GpppG	76±2	61±12	76±10	1.41±0.26
-	m^{7}GpppG	nd[b]	nd	nd	1±0
-	ApppG	nd	nd	nd	0.12±0.01

[a] normalised to m^{7}GpppG;

[b] not determined